TABLE 1 (Continued)

Clone designation	CA mutation(s)[b]	Growth potential[c]
L6I-LSDQA	L6I, M94L, R98S, G114Q, Q178A	++++
DLSDQA	E71D, M94L, R98S, G114Q, Q178A	+++
L6I-DLSDQA	L6I, E71D, M94L, R98S, G114Q, Q178A	+++
LSDQAV	M94L, R98S, G114Q, Q178A, P206V	++++
L6I-LSDQAV	L6I, M94L, R98S, G114Q, Q178A, P206V	++++
YQ-LSDQAV	Q50Y, T54Q, M94L, R98S, G114Q, Q178A, P206V	−
DLSDQAV	E71D, M94L, R98S, G114Q, Q178A, P206V	+++
L6I-DLSDQAV	L6I, E71D, M94L, R98S, G114Q, Q178A, P206V	+++
Mutants of the β-hairpin domain		
DdN5	N5 deletion	−
DdN5-Y	N5 deletion, T117Y	−
SDdN5	N5 deletion, R98S	−
SDdN5-Y	N5 deletion, R98S, T117Y	−
DQdN5-Y	N5 deletion, G114Q, T117Y	−
SDQdN5	N5 deletion, R98S, G114Q	−
SDQdN5-Y	N5 deletion, R98S, G114Q, T117Y	−
LSDQdN5	N5 deletion, M94L, R98S, G114Q	−
LSDQdN5-Y	N5 deletion, M94L, R98S, G114Q, T117Y	−
QIG-S	NLQ5-7QIG, R98S	−
QIG-SDQ	NLQ5-7QIG, R98S, G114Q	−
QIG-LSDQ	NLQ5-7QIG, M94L, R98S, G114Q	−
GGN-S	QGQ7-9GGN, R98S	−
GGN-LSDQ	QGQ7-9GGN, M94L, R98S, G114Q	−
GGN-YQ-LSDQ	QGQ7-9GGN, Q50Y, T54Q, M94L, R98S, G114Q	−
L6I-YQ-LSDQ	L6I, Q50Y, T54Q, M94L, R98S, G114Q	−
IL-LSDQA	L6I, Q13L, M94L, R98S, G114Q, Q178A	−
IL-Y-LSDQA	L6I, Q13L, M94L, R98S, G114Q, T117Y, Q178A	−
IN-LSDQA	L6I, Q9N, M94L, R98S, G114Q, Q178A	−
IN-Y-LSDQA	L6I, Q9N, M94L, R98S, G114Q, T117Y, Q178A	−
IY-Y-LSDQA	L6I, M10Y, M94L, R98S, G114Q, T117Y, Q178A	−
INY-LSDQA	L6I, Q9N, M10Y, M94L, R98S, G114Q, Q178A	−
INY-Y-LSDQA	L6I, Q9N, M10Y, M94L, R98S, G114Q, T117Y, Q178A	−
INL-LSDQA	L6I, Q9N, Q13L, M94L, R98S, G114Q, Q178A	−
INL-Y-LSDQA	L6I, Q9N, Q13L, M94L, R98S, G114Q, T117Y, Q178A	−
IYL-LSDQA	L6I, M10Y, Q13L, M94L, R98S, G114Q, Q178A	−
IYL-Y-LSDQA	L6I, M10Y, Q13L, M94L, R98S, G114Q, T117Y, Q178A	−
INYL-LSDQA	L6I, Q9N, M10Y, Q13L, M94L, R98S, G114Q, Q178A	−
INYL-Y-LSDQA	L6I, Q9N, M10Y, Q13L, M94L, R98S, G114Q, T117Y, Q178A	−
Q13L-LSDQ	Q13L, M94L, R98S, G114Q	−
Q13L-Y-LSDQ	Q13L, M94L, R98S, G114Q, T117Y	−
Q13L-LSDQA	Q13L, M94L, R98S, G114Q, Q178A	−
Q13L-Y-LSDQA	Q13L, M94L, R98S, G114Q, T117Y, Q178A	−

[a] MN4Rh-3 CA was constructed by replacing the CypA-binding loop and H6/7L of HIV-1_{NL4-3} CA with the corresponding regions of SIVmac239 CA and by the additional introduction of a Q110D mutation (Fig. 1) (19, 24).

[b] Amino acid number in MN4Rh-3 CA.

[c] Viral growth potential in M1.3S cells. ++++, grows similarly to MN4/LSDQ; +++, grows more efficiently than MN4Rh-3; ++, grows similarly to MN4Rh-3; +, grows more poorly than MN4Rh-3; −, undetectable during the observation period.

clones here, except for MN4Rh-3, exhibited a tendency to have a higher level of resistance to CyM-TRIM5α than to RhM-TRIM5α (Fig. 4). It has been shown that TRIM5α proteins encoded by *TRIM5*^{TFP} are more restrictive to virus infection than are those encoded by *TRIM5*^{Q} (40). The observed tendency for TRIM5α resistance may be due to the difference between RhM-TRIM5α (*TRIM5*^{TFP}) and CyM-TRIM5α (*TRIM5*^{Q}) used in the assay. These results indicate that the enhancement of viral growth in M1.3S cells by CA alterations depends, at least in part, on the increased resistance to TRIM5α.

Virus replication capability in macaque PBMCs with different *TRIM5* alleles reflects the TRIM5α resistance of HIV-1mt clones. We have previously shown that MN4Rh-3 replicates well in *TRIM5α/TRIM5CypA* heterozygous CyM PBMCs/individuals, but its replication was restricted in *TRIM5α* homozygous CyM PBMCs/individuals (19, 24). To confirm the effect of the increased resistance of MN4/LSDQ and MN5/LSDQ against macaque TRIM5α on viral replication, we examined their replication potential relative to that of MN4Rh-3 and MN5Rh-3 in *TRIM5α/TRIM5CypA* heterozygous or *TRIM5α* homozygous macaque PBMCs.

First, we compared viral growth potentials of the clones in CyM PBMCs (Fig. 5A). Growth kinetics of MN4Rh-3 and MN4/LSDQ were similar in *TRIM5α/TRIM5CypA* heterozygous CyM

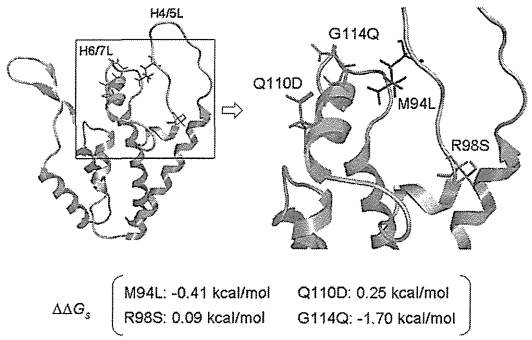

FIG 3 Structural analysis of the HIV-1mt CA NTD. A molecular model of the HIV-1mt CA NTD was constructed by homology modeling and refined as described previously (19). Single-point mutations were generated on the CA model, and ensembles of protein conformations were generated by using the LowMode MD module in MOE (Chemical Computing Group Inc., Quebec, Canada) to calculate average stability by using Boltzmann distribution. The stability scores ($\Delta\Delta G_s$) of the structures refined by energy minimization were obtained through the stability scoring function of the Protein Design application and are indicated below the structural model.

PBMCs. In contrast, the replication efficiency of MN4/LSDQ was markedly enhanced in *TRIM5*α homozygous CyM PBMCs relative to that of MN4Rh-3 (Fig. 5A). Similar results were obtained with RhM PBMCs. MN4Rh-3 exhibited growth kinetics comparable to those of MN4/LSDQ in *TRIM5*α/*TRIM5CypA* heterozygous RhM PBMCs (Fig. 5B). In *TRIM5*α homozygous RhM PBMCs, MN5/LSDQ replicated much more efficiently than MN5Rh-3 (Fig. 5C). CXCR4-tropic HIV-1mt clones (MN4 series) were found to exhibit a higher growth ability than CCR5-tropic HIV-1mt clones (MN5 series) in both M1.3S cells and macaque PBMCs (Fig. 2D and 5B and C) and were therefore used for experiments thereafter. In sum, the replication potential of TRIM5α-resistant HIV-1mt clones (MN4/LSDQ and MN5/LSDQ) markedly increased in *TRIM5*α homozygous PBMCs but was similar to that of TRIM5CypA-resistant/TRIM5α-sensitive clones (MN4Rh-3 and MN5Rh-3) in *TRIM5*α/*TRIM5CypA* heterozygous PBMCs. These results suggest that M94L/R98S/G114Q mutations in MN4Rh-3 CA largely contribute to the acquisition of TRIM5α resistance.

HIV-1 Vpu gains the ability to specifically counteract macaque tetherin by replacing its TM domain with the corresponding region of SIVgsn166 Vpu. Tetherin as well as TRIM5 proteins are important anti-HIV-1 factors in macaque cells (4, 8, 10), but the HIV-1mt clones constructed so far do not display macaque tetherin antagonism due to Vpu derived from HIV-1_{NL4-3}. It has been shown that Vpu from SIVmon/mus/gsn can antagonize macaque tetherin but not human tetherin (26). To confer the ability to counteract macaque tetherin on HIV-1mt clones, we modified the *vpu* gene. The sequence of the cytoplasmic domain of HIV-1 Vpu partially overlaps the 5′-end sequence of Env, and the TM domain of Vpu is a key region for species-specific tetherin antagonism (22). Thus, we constructed Vpu clones that contain SIVmon/mus/gsn TM and HIV-1mt cytoplasmic domains (Fig. 6A). First, RhM tetherin antagonism of various Vpu clones was analyzed by Vpu *trans*-complementation assays for virion release (Fig. 6B). 293T cells were cotransfected with a *vpu*-deficient HIV-1mt clone (MN4Rh-3-ΔU), an RhM tetherin expression vector (pCIneo-RhM tetherin), and various Vpu constructs, and virion production from cells on day 2 posttransfection was measured. While MN4Rh-3-ΔU released progeny virions efficiently upon transfection without RhM tetherin expression, its virion production was significantly inhibited in the presence of RhM tetherin. Although this reduction was not rescued by HIV-1_{NL4-3} Vpu, SIVmon/mus/gsn Vpu restored it to some extent, consistent with a previous report (26). Of the SIV/HIV-1 chimeric Vpu proteins, gsnTM-Vpu appeared to be somewhat better than the others and was therefore used thereafter.

Next, we examined the ability of HIV-1_{NL4-3} Vpu and gsnTM-Vpu to downregulate cell surface CD4 and tetherin (Fig. 6C). MAGI, LLC-MK2, and HEp2 cells were used for analysis of CD4,

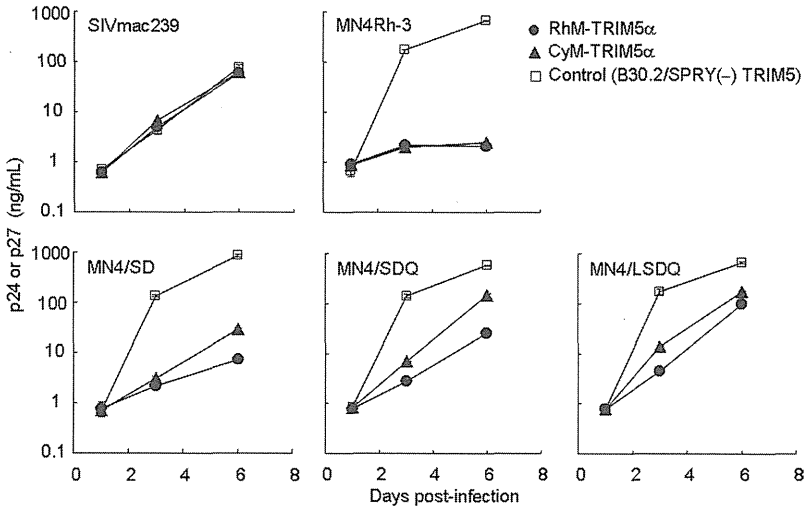

FIG 4 Susceptibility of SIVmac239 and various HIV-1mt clones to macaque TRIM5α. Human MT4 cells (10^5) were infected with recombinant SeV expressing RhM-TRIM5α (*TRIM5*^{TPP}), CyM-TRIM5α (*TRIM5*^{Q}), or B30.2/SPRY(−) TRIM5. Nine hours after infection, cells were superinfected with 20 ng (Gag-p24) of various HIV-1mt clones or 20 ng (Gag-p27) of SIVmac239. Virus replication was monitored by the amount of Gag-p24 from HIV-1mt clones or Gag-p27 from SIVmac239 in the culture supernatants. Error bars show actual fluctuations between duplicate samples. Representative data from two independent experiments are shown.

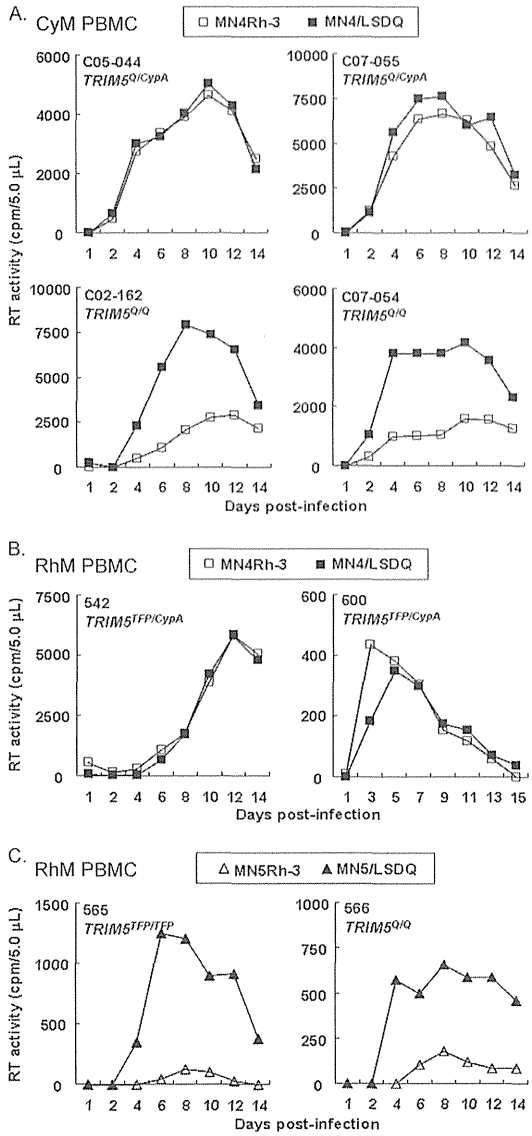

FIG 5 Growth kinetics of HIV-1mt clones with a distinct CA in macaque PBMCs. (A) Infection of PBMCs from four *TRIM5α/TRIM5CypA* heterozygous or *TRIM5α* homozygous CyM individuals. (B and C) Infection of PBMCs from four RhM individuals with different *TRIM5* alleles. For infection, input viruses were prepared from 293T cells transfected with the proviral clones indicated, and equal amounts (2.5×10^6 RT units) were used to spin infect PBMCs (2×10^6 cells). Virus replication was monitored by RT activity released into the culture supernatants. Monkey identification numbers are indicated in each panel.

RhM tetherin, and human tetherin, respectively. Cells were transfected with Vpu-green fluorescent protein (GFP) bicistronic expression plasmids and subjected to flow cytometry analysis on day 2 posttransfection. While both HIV-1_{NL4-3} Vpu and gsnTM-Vpu significantly decreased cell surface CD4 levels, the RhM tetherin level was reduced by gsnTM-Vpu but not by HIV-1_{NL4-3} Vpu. Similar results were obtained for MK.P3(F) cells expressing endogenous CyM tetherin (data not shown). In contrast, HIV-1_{NL4-3} Vpu but not gsnTM-Vpu downmodulated cell surface human tetherin. These results show that the transfer of the SIVgsn166 Vpu TM domain to HIV-1 Vpu is sufficient to confer the ability to specifically antagonize macaque tetherin on viruses.

gsnTM-Vpu in the context of proviral genome functions in macaque cells. To ask if gsnTM-Vpu is functional in the proviral context, we generated an HIV-1mt clone encoding gsnTM-Vpu (MN4/LSDQgtu) (Fig. 1 and 7A). Interestingly, it has been shown that Vpu of HIV-1 composed of HIV-1_{DH12} TM and HIV-1_{NL4-3} cytoplasmic domains counteracts macaque tetherin (22). We thus constructed another HIV-1mt clone, MN4/LSDQdtu, that has chimeric Vpu, as described above (Fig. 7A).

To examine the species-specific tetherin antagonism of these proviral clones, we carried out virion release assays in the presence of RhM or human tetherin (Fig. 7B). Using SIVmac239 Nef as a control antagonist against macaque tetherin (52, 53), the anti-macaque tetherin activities of MN4/LSDQ, MN4/LSDQdtu, and MN4/LSDQgtu were comparatively analyzed. As described above, SIVmac239 Nef exhibited the ability to specifically antagonize macaque tetherin. As expected, virion production of MN4/LSDQ and its *vpu*-deficient clone was similarly restricted in the presence of RhM tetherin, and MN4/LSDQ displayed a higher level of virion production than that of its *vpu*-deficient clone in the presence of human tetherin, indicating its specific antagonism to human tetherin. Also, as expected from a previous report (22), MN4/LSDQdtu showed both RhM and human tetherin antagonism, although its anti-RhM tetherin activity was relatively low. Strikingly, virion production levels of MN4/LSDQgtu in the presence of RhM/human tetherin were similar to those of SIVmac239. This indicates that MN4/LSDQgtu has specifically strong anti-RhM tetherin activity, as is the case for SIVmac239. To see if various Vpu proteins function during viral replication in macaque cells, we determined the growth properties of various HIV-1mt clones carrying distinct Vpu proteins. Although the effect of *vpu* deletion is virologically small, *vpu*-deficient viruses are readily distinguishable from the parental wild-type virus by comparative kinetic analysis of viral growth (22, 29). As shown in Fig. 7C, while MN4/LSDQ and MN4/LSDQdtu exhibited growth kinetics similar to those of their respective *vpu*-deficient clones, *vpu*-deficient MN4/LSDQgtu grew significantly more poorly than its parental virus. Taken together, it can be concluded that MN4/LSDQgtu Vpu but not MN4/LSDQ Vpu functions during viral replication in M1.3S cells. However, the functionality of MN4/LSDQdtu Vpu in macaque cells was not clear in the viral growth kinetics here. Although there are some possible explanations, the relatively low anti-RhM tetherin activity of MN4/LSDQdtu (see the results in Fig. 7B) could account for this observation.

Although the tertiary structure of the HIV-1 Vpu TM domain has been determined by NMR (38), the structure of the TM domain from SIV Vpu has not been solved to date. To investigate how replacement of the Vpu TM domain could lead to changes in TM structure, we constructed structural models of Vpu TM domains of MN4/LSDQ, MN4/LSDQdtu, and MN4/LSDQgtu (Fig. 7D). This modeling study revealed that the types of amino acid residues corresponding to the crucial residues (54) in HIV-1 Vpu for binding with human tetherin are similar between MN4/LSDQ and MN4/LSDQdtu, whereas they are often different in MN4/LSDQgtu. In addition, their steric locations in the helices are also similar between MN4/LSDQ and MN4/LSDQdtu, whereas they are very different in MN4/LSDQgtu. Finally, angles between the

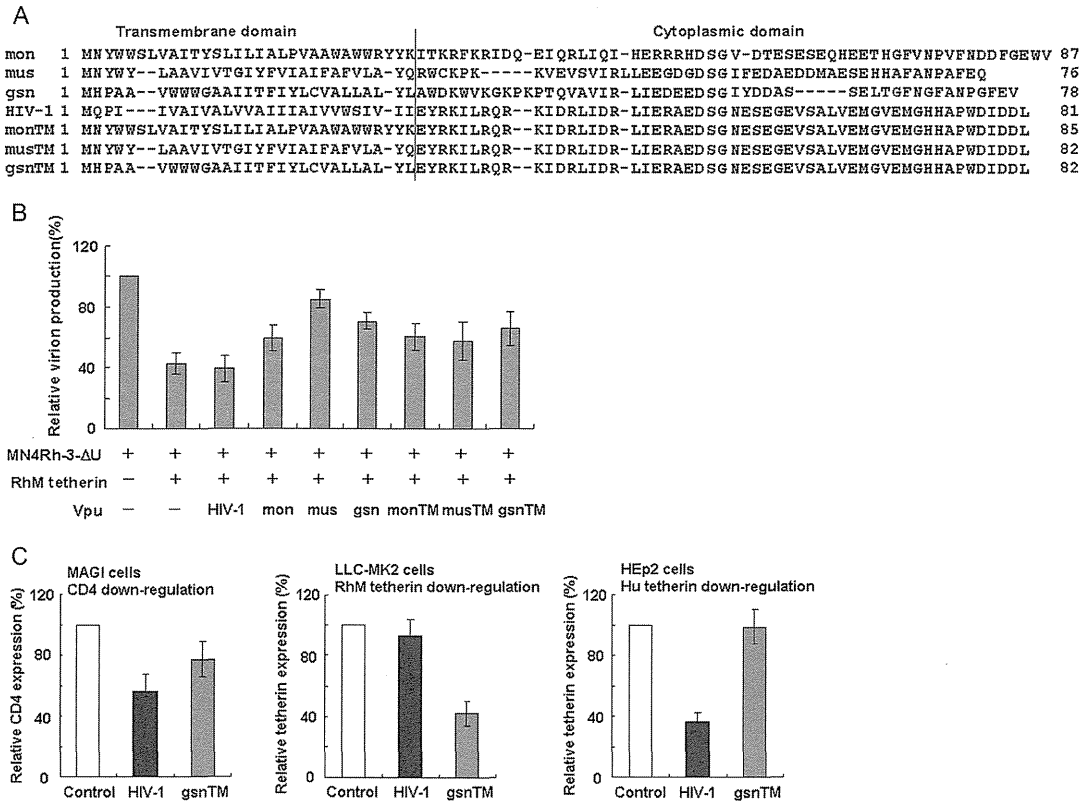

FIG 6 Generation of SIV/HIV-1 chimeric Vpu proteins resistant to macaque tetherin. (A) Amino acid sequences of various Vpu proteins. Alignments of the sequences and the boundary between TM/cytoplasmic domains are shown based on previously reported information (26). mon, SIVmonCML1 (GenBank accession number AY340701); mus, SIVmus1085 (GenBank accession number AY340700); gsn, SIVgsn166 (GenBank accession number AF468659); HIV-1, NL4-3 (32). HIV-1mt clones (MN4 series) have *vpu* genes identical to that of NL4-3. monTM-, musTM-, and gsnTM-Vpu were constructed by fusing each TM domain of SIVmon/mus/gsn Vpu with the cytoplasmic domain of HIV-1_{NL4-3} Vpu. (B) RhM tetherin antagonism by various Vpu proteins. 293T cells were cotransfected with a *vpu*-deficient proviral clone (MN4Rh-3-ΔU), pCIneo-RhM tetherin, and various pSG-VpucFLAG constructs. On day 2 posttransfection, virion production in the culture supernatants was determined by RT assays. Virion production levels relative to that of MN4Rh-3-ΔU in the absence of RhM tetherin were calculated, and mean values of three independent experiments are shown with the standard deviations. (C) Downregulation of cell surface CD4 and tetherin by HIV-1_{NL4-3} Vpu or gsnTM-Vpu. MAGI, LLC-MK2, and HEp2 cells were used to determine the downregulation of CD4, RhM tetherin, and human (Hu) tetherin by Vpu, respectively. Cells were transfected with the pIRES-hrGFP (control), pIRES-HIV-1 Vpu-hrGFP, or pIRES-gsnTM-Vpu-hrGFP construct. On day 2 posttransfection, cells were stained for cell surface CD4 or tetherin and analyzed by two-color flow cytometry. Values presented are CD4 or tetherin fluorescence intensities of GFP-positive cells relative to that of the control. Mean values ± standard deviations of three independent experiments are shown.

central lines of the helices are similar between MN4/LSDQ and MN4/LSDQdtu, whereas they are different in MN4/LSDQgtu. These results suggest the possibility that the structural properties of the tetherin interaction surface of the MN4/LSDQgtu Vpu TM domain are very different from those of the Vpu TM domains of MN4/LSDQ and MN4/LSDQdtu. Further studies are necessary to verify this issue.

RhM APOBEC3-, TRIM5α-, and tetherin-resistant HIV-1mt clone MN4/LSDQgtu replicates comparably to SIVmac239 in RhM PBMCs. Here we constructed distinct HIV-1mt clones with respect to their resistance to RhM TRIM5α and tetherin: TRIM5α- and tetherin-susceptible MN4Rh-3, TRIM5α-resistant but tetherin-susceptible MN4/LSDQ, and TRIM5α- and tetherin-resistant MN4/LSDQgtu. Of note, all these clones are RhM APOBEC3 resistant (see Fig. 1 for their genomes). To investigate the effect of the increased resistance to these macaque restriction factors, various viruses were examined for their growth potential in PBMCs from four *TRIM5α* homozygous RhM individuals. As shown in Fig. 8, SIVmac239, a comparative standard virus in macaque cells, replicated constantly in all PBMC preparations. The growth potentials in the RhM PBMCs of the HIV-1mt clones tested markedly and stably differed. As a likely result of RhM TRIM5α-resistant Gag-CA, MN4/LSDQ replicated much more efficiently than MN4Rh-3. By virtue of RhM tetherin-resistant Vpu, MN4/LSDQgtu grew significantly better than MN4/LSDQ. Essentially the same results for HIV-1mt growth kinetics were obtained in M1.3S cells. The M1.3S cell line and macaque PBMCs always responded similarly to various SIVs/HIVs (our unpublished observations). Moreover, by comparing the peak day of viral growth kinetics and the peak level itself, MN4/LSDQgtu was shown here to have the ability to replicate comparably to SIVmac239 in RhM PBMCs, except for one preparation (from monkey 565) (Fig. 8). The results show that the increased resistance to macaque restriction factors correlates well with the enhanced viral growth potential. In sum, MN4/LSDQgtu, which exhibits resistance to known major restriction factors (APOBEC3, TRIM5, and tetherin

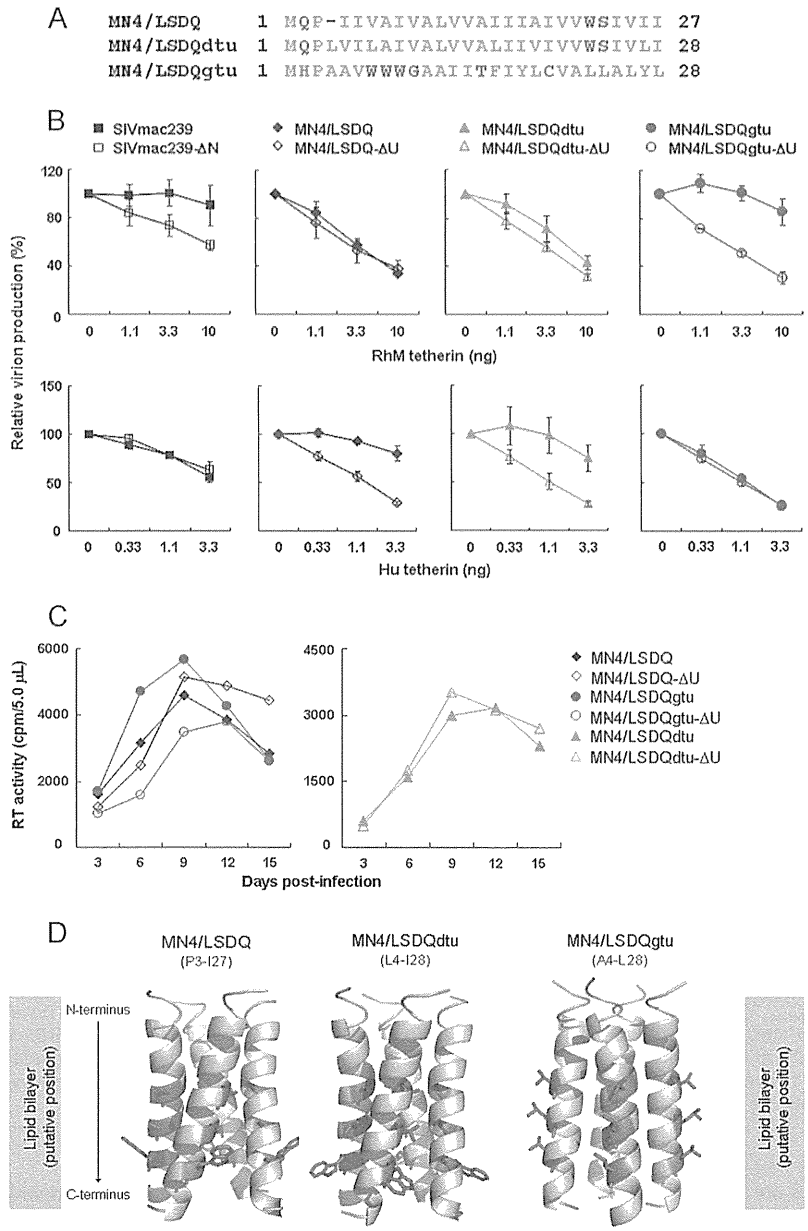

FIG 7 Effects of various Vpu proteins carrying a different TM domain on tetherin antagonism and HIV-1mt replication in macaque cells. (A) Alignment of amino acid sequences of the Vpu TM domain in each HIV-1mt clone. MN4/LSDQ, MN4/LSDQdtu, and MN4/LSDQgtu encode the Vpu TM domain derived from HIV-1_{NL4-3} (32), HIV-1_{DH12} (22), and SIVgsn166 (GenBank accession number AF468659), respectively. (B) Species-specific tetherin antagonism by SIVmac239 and various HIV-1mt clones carrying different Vpu proteins. SIVmac239 (MA239N) and its *nef*-deficient clone (MA239N-ΔN) were used as positive controls for RhM tetherin resistance. 293T cells were cotransfected with proviral clones and the indicated amounts of the pCIneo-RhM tetherin or pCIneo-Human tetherin expression vector. On day 2 posttransfection, virion production was determined by RT activity released into the culture supernatants. Values are presented as RT activity of each sample relative to that of each proviral clone without tetherin expression. Mean values ± standard deviations of three independent experiments are shown. ΔU, *vpu* deficient; Hu, human. (C) Growth kinetics of various HIV-1mt clones and their *vpu*-deficient clones in M1.3S cells. Viruses were prepared from 293T cells transfected with the indicated proviral clones, and equal amounts (5×10^5 RT units) were inoculated into M1.3S cells (2×10^5 cells). Virus replication was monitored by RT activity released into the culture supernatants. Representative data from three independent experiments are shown. (D) Structural modeling of Vpu TM domains of MN4/LSDQ, MN4/LSDQdtu, and MN4/LSDQgtu. Predicted models are shown in a ribbon representation. Amino acid residues corresponding to the residues in HIV-1 Vpu crucial for binding with human tetherin (54) are highlighted in a red stick representation. Crucial residues in Vpu TM domains of MN4/LSDQ, MN4/LSDQdtu, and MN4/LSDQgtu are A14/A18/W22, A15/V19/W23, and T15/L19/L23, respectively. TM regions analyzed (see panel A for amino acid sequences) are indicated in parentheses.

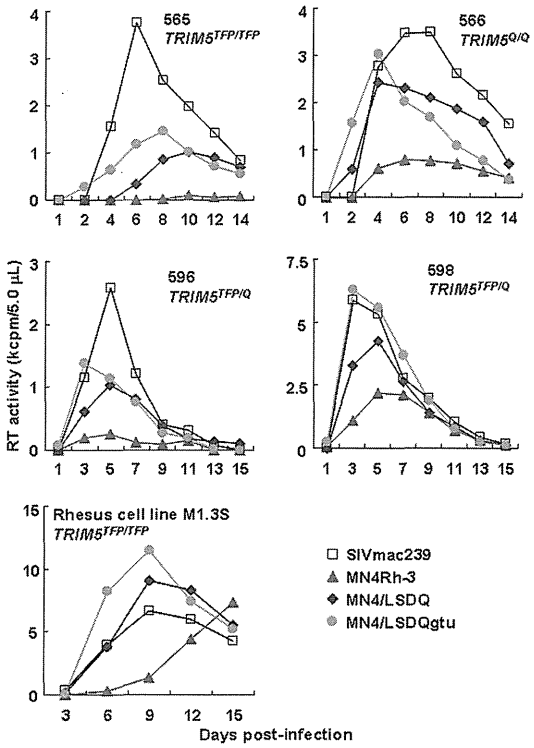

FIG 8 Growth kinetics of SIVmac239 and various HIV-1mt clones in *TRIM5α* homozygous RhM PBMCs. PBMCs were prepared from four RhM individuals with the different *TRIM5* alleles indicated. Viruses were prepared from 293T cells transfected with the indicated proviral clones, and equal amounts (2.5×10^6 RT units) were used to spin infect PBMCs (2×10^6 cells). As a control experiment, rhesus M1.3S cells (2×10^5) were infected with equal amounts of viruses (5×10^5 RT units). Virus replication was monitored by RT activity released into the culture supernatants. Monkey identification numbers are indicated in each panel.

proteins), is the best HIV-1mt clone generated so far, replicating with an efficiency similar to that of SIVmac239 in RhM cells.

DISCUSSION

In this study, we generated a novel HIV-1mt clone, designated MN4/LSDQgtu, that exhibits resistance to RhM TRIM5α and tetherin in addition to APOBEC3 proteins (Fig. 1). By sequence homology- and structure-guided CA mutagenesis and by screening the multicycle growth potential of CA mutant viruses in M1.3S cells, we successfully obtained viruses with enhanced replication efficiency in macaque cells as well as increased macaque TRIM5α resistance (Fig. 2 to 5). The transfer of the TM domain of SIVgsn166 Vpu into the corresponding region of HIV-1mt Vpu conferred the ability to specifically counteract macaque tetherin on the virus (Fig. 6 and 7). Furthermore, the increased resistance to both RhM TRIM5α and tetherin contributed to the viral growth enhancement in RhM PBMCs (Fig. 8).

During the preparation of this paper, McCarthy et al. reported several key residues in SIVmac239 CA involved in the interaction with RhM TRIM5α by genetic and structural analysis (55). Interestingly, the HIV-1mt CA amino acid residues identified in this study as being the elements responsible for the increased resistance to RhM TRIM5α (M94L/R98S/Q110D/G114Q) were included in those residues. McCarthy et al. reported that H4/5L and helix 6 of SIVmac239 CA also affect TRIM5α sensitivity (55). In the construction process for our HIV-1mt clones, we found that the CA elements involved in the interaction with RhM TRIM5α are the CypA-binding loop within H4/5L, H6/7L, M94L/R98S within H4/5L, and Q110D/G114Q in helix 6 (18–20, 56; this study). Of the substitutions identified in this study, R98S was the primary residue to increase TRIM5α resistance and improve viral growth in macaque cells. It was also shown that the TRIM5α (*TRIM5*^{TFP})-susceptible SIVsmE543-3 clone acquires an adaptive R97S change in CA (corresponding to R98S in MN4Rh-3 CA) to evade TRIM5α (*TRIM5*^{TFP}) restriction during viral replication in RhM individuals (40). In TRIM5α-sensitive CA, R98S may be a key residue contributing to the evasion of TRIM5α restriction. Together, these results suggest that CA elements critical for recognition by TRIM5α may be conserved among primate lentiviruses. The RhM TRIM5α-resistant HIV-1 CA constructed in this study would be useful to define how TRIM5α recognizes CA. On the other hand, MN4/LSDQ appeared not to evade TRIM5α restriction completely, as SIVmac239 did (Fig. 4). In this regard, since it has been shown that the N-terminal β-hairpin domain in the retroviral CA contributes to circumventing TRIM5α (36, 55, 57), we constructed various HIV-1mt clones carrying mutations in the domain (Table 1). However, except for the L6I substitution, none of the clones were infectious (Table 1). A further CA modification(s) may be necessary for complete evasion of TRIM5α restriction.

Accumulating evidence has shown that tetherin is an important cellular restriction factor that affects the replication, adaptation, and evolution of primate immunodeficiency viruses (4, 26). Its negative effect on viral replication is certainly observed in cultured cell lines and primary cells but is not so evident relative to those of APOBEC3 and TRIM5 proteins (10). Also, in the present study, RhM tetherin-resistant Vpu significantly contributed to viral growth enhancement but not as much as TRIM5α-resistant CA (Fig. 7 and 8). However, tetherin has been suggested to play an important effector role in antiretroviral activity induced by alpha interferon (58–60). Also, it has been shown that the pathogenic revertant virus from nonpathogenic *nef*-deficient virus acquires tetherin antagonism by adaptive mutations in the gp41 subunit of Env (61). Therefore, the ability of HIV-1mt clones to antagonize RhM tetherin may be very important for optimal replication and pathogenesis in RhM individuals. In this regard, it has been described that naturally occurring polymorphisms in RhM tetherin sequences are present (30, 31, 61). Although whether these variations have some appreciable effects on viral replication *in vitro* is undetermined, the relationship between tetherin polymorphisms and the viral replication level *in vivo* (animals)/viral pathogenic activity *in vivo* may be a major issue to address and remains to be extensively analyzed. It would be intriguing to elucidate how the viral accessory protein Vpu *in vitro* is associated with the *in vivo* replicative and pathogenic properties of HIV-1 (22).

We constructed an MN4/LSDQgtu clone resistant to the known major restriction factors (APOBEC3, TRIM5, and tetherin proteins) in RhM cells. The growth potential of MN4/LSDQgtu was similar to that of SIVmac239 in most RhM PBMC preparations (Fig. 8). It was shown previously that the *in vivo* replication of SIV is predictable from the virus susceptibility of PBMCs (62, 63). Also, in a series of our studies, the better our HIV-1mt clones grew in PBMCs, the better they grew in the monkeys (20, 24, 64).

Thus, it is expected that MN4/LSDQgtu will grow much better in RhM individuals, at least in the early infection phase, than the other HIV-1mt clones constructed. As reported previously, the replication of HIV-1 derivatives in infected macaques was eventually controlled, and no disease was induced in the animals (16, 20, 21, 24, 64). It has been suggested that the replication ability of primate lentiviruses in unusual hosts is more severely affected, via an interferon-induced antiviral state mediated by unidentified species-specific factors, than that in natural hosts (23). Moreover, there are the other significant issues to be considered, such as viral coreceptor tropism (CXCR4 versus CCR5), the diversity in viral growth properties (HIV-1 versus SIVmac), and the difference in host immune responses (human versus RhM) (9, 65–67). Most importantly, CCR5-tropic but not CXCR4-tropic clones have been found to be appropriate as input viruses to experimentally infect RhMs for various HIV-1 model studies *in vivo* (65–67). Although MN4/LSDQgtu is a CXCR4-tropic virus, it has clear potential for the establishment of a model system. MN4/LSDQgtu can be changed to a pathogenic CCR5-tropic virus through *in vitro* and *in vivo* approaches, as well documented by previous SHIV studies (68–70). It is also possible to generate entirely new CCR5-tropic HIV-1mt clones other than MN4/LSDQgtu derivatives on the basis of the key findings for Gag-CA and Vpu-TM in this study.

Our study here describes the generation and characterization of a novel HIV-1 derivative minimally chimeric with SIVs. Several infection model systems using distinct viruses and nonhuman primates are now available. It is important to define common and unique characteristics of each virus-host interaction based on the results obtained from various experimental approaches, including SIV/natural host and SIVmac/RhM, SHIV/RhM, and HIV-1mt/RhM infection systems. Such efforts would shed light on a better understanding of HIV-1/human infection and HIV-1 pathogenesis.

ACKNOWLEDGMENTS

This study was supported in part by a grant from the Ministry of Health, Labor and Welfare of Japan (Research on HIV/AIDS project no. H23-003).

We thank Kazuko Yoshida for editorial assistance.

We declare that no competing interests exist.

REFERENCES

1. **Kirchhoff F.** 2010. Immune evasion and counteraction of restriction factors by HIV-1 and other primate lentiviruses. Cell Host Microbe **8**:55–67.
2. **Sharp PM, Hahn BH.** 2011. Origins of HIV and the AIDS pandemic. Cold Spring Harb. Perspect. Med. **1**:a006841. doi:10.1101/cshperspect.a006841.
3. **Shibata R, Sakai H, Kawamura M, Tokunaga K, Adachi A.** 1995. Early replication block of human immunodeficiency virus type 1 in monkey cells. J. Gen. Virol. **76**:2723–2730.
4. **Blanco-Melo D, Venkatesh S, Bieniasz PD.** 2012. Intrinsic cellular defenses against human immunodeficiency viruses. Immunity **37**:399–411.
5. **Harris RS, Hultquist JF, Evans DT.** 2012. The restriction factors of human immunodeficiency virus. J. Biol. Chem. **287**:40875–40883.
6. **Malim MH, Bieniasz PD.** 2012. HIV restriction factors and mechanisms of evasion. Cold Spring Harb. Perspect. Med. **2**:a006940. doi:10.1101/cshperspect.a006940.
7. **Hatziioannou T, Evans DT.** 2012. Animal models for HIV/AIDS research. Nat. Rev. Microbiol. **10**:852–867.
8. **Nomaguchi M, Doi N, Fujiwara S, Adachi A.** 2011. Macaque-tropic HIV-1 derivatives: a novel experimental approach to understand viral replication and evolution *in vivo*, p 325–348. *In* Chang T.Y.-L. (ed), HIV-host interactions. InTech, Rijeka, Croatia. http://www.intechopen.com/books/hiv-host-interactions/macaque-tropic-hiv-1-derivatives-a-novel-experimental-approach-to-understand-viral-replication-and-e.
9. **Shedlock DJ, Silvestri G, Weiner DB.** 2009. Monkeying around with HIV vaccines: using rhesus macaques to define 'gatekeepers' for clinical trials. Nat. Rev. Immunol. **9**:717–728.
10. **Nomaguchi M, Doi N, Matsumoto Y, Sakai Y, Fujiwara S, Adachi A.** 2012. Species tropism of HIV-1 modulated by viral accessory proteins. Front. Microbiol. **3**:267. doi:10.3389/fmicb.2012.00267.
11. **Holmes RK, Malim MH, Bishop KN.** 2007. APOBEC-mediated viral restriction: not simply editing? Trends Biochem. Sci. **32**:118–128.
12. **Malim MH, Emerman M.** 2008. HIV-1 accessory proteins—ensuring viral survival in a hostile environment. Cell Host Microbe **3**:388–398.
13. **Grütter MG, Luban J.** 2012. TRIM5 structure, HIV-1 capsid recognition, and innate immune signaling. Curr. Opin. Virol. **2**:142–150.
14. **Nakayama EE, Shioda T.** 2010. Anti-retroviral activity of TRIM5 alpha. Rev. Med. Virol. **20**:77–92.
15. **Douglas JL, Gustin JK, Viswanathan K, Mansouri M, Moses AV, Früh K.** 2010. The great escape: viral strategies to counter BST-2/tetherin. PLoS Pathog. **6**:e1000913. doi:10.1371/journal.ppat.1000913.
16. **Hatziioannou T, Ambrose Z, Chung NP, Piatak M, Jr, Yuan F, Trubey CM, Coalter V, Kiser R, Schneider D, Smedley J, Pung R, Gathuka M, Estes JD, Veazey RS, KewalRamani VN, Lifson JD, Bieniasz PD.** 2009. A macaque model of HIV-1 infection. Proc. Natl. Acad. Sci. U. S. A. **106**:4425–4429.
17. **Hatziioannou T, Princiotta M, Piatak M, Jr, Yuan F, Zhang F, Lifson JD, Bieniasz PD.** 2006. Generation of simian-tropic HIV-1 by restriction factor evasion. Science **314**:95. doi:10.1126/science.1130994.
18. **Kamada K, Igarashi T, Martin MA, Khamsri B, Hatcho K, Yamashita T, Fujita M, Uchiyama T, Adachi A.** 2006. Generation of HIV-1 derivatives that productively infect macaque monkey lymphoid cells. Proc. Natl. Acad. Sci. U. S. A. **103**:16959–16964.
19. **Nomaguchi M, Yokoyama M, Kono K, Nakayama EE, Shioda T, Saito A, Akari H, Yasutomi Y, Matano T, Sato H, Adachi A.** 2013. Gag-CA Q110D mutation elicits TRIM5-independent enhancement of HIV-1mt replication in macaque cells. Microbes Infect. **15**:56–65.
20. **Saito A, Nomaguchi M, Iijima S, Kuroishi A, Yoshida T, Lee YJ, Hayakawa T, Kono K, Nakayama EE, Shioda T, Yasutomi Y, Adachi A, Matano T, Akari H.** 2011. Improved capacity of a monkey-tropic HIV-1 derivative to replicate in cynomolgus monkeys with minimal modifications. Microbes Infect. **13**:58–64.
21. **Thippeshappa R, Polacino P, Yu Kimata MT, Siwak EB, Anderson D, Wang W, Sherwood L, Arora R, Wen M, Zhou P, Hu SL, Kimata JT.** 2011. Vif substitution enables persistent infection of pig-tailed macaques by human immunodeficiency virus type 1. J. Virol. **85**:3767–3779.
22. **Shingai M, Yoshida T, Martin MA, Strebel K.** 2011. Some human immunodeficiency virus type 1 Vpu proteins are able to antagonize macaque BST-2 *in vitro* and *in vivo*: Vpu-negative simian-human immunodeficiency viruses are attenuated *in vivo*. J. Virol. **85**:9708–9715.
23. **Bitzegeio J, Sampias M, Bieniasz PD, Hatziioannou T.** 2013. Adaptation to the interferon-induced antiviral state by human and simian immunodeficiency viruses. J. Virol. **87**:3549–3560.
24. **Saito A, Nomaguchi M, Kono K, Iwatani Y, Yokoyama M, Yasutomi Y, Sato H, Shioda T, Sugiura W, Matano T, Adachi A, Nakayama E, Akari H.** 2013. *TRIM5* genotypes in cynomolgus monkeys primarily influence inter-individual diversity in susceptibility to monkey-tropic human immunodeficiency virus type 1. J. Gen. Virol. **94**:1318–1324.
25. **Doi N, Fujiwara S, Adachi A, Nomaguchi M.** 2011. Rhesus M1.3S cells suitable for biological evaluation of macaque-tropic HIV/SIV clones. Front. Microbiol. **2**:115. doi:10.3389/fmicb.2011.00115.
26. **Sauter D, Schindler M, Specht A, Landford WN, Münch J, Kim KA, Votteler J, Schubert U, Bibollet-Ruche F, Keele BF, Takehisa J, Ogando Y, Ochsenbauer C, Kappes JC, Ayouba A, Peeters M, Learn GH, Shaw G, Sharp PM, Bieniasz P, Hahn BH, Hatziioannou T, Kirchhoff F.** 2009. Tetherin-driven adaptation of Vpu and Nef function and the evolution of pandemic and nonpandemic HIV-1 strains. Cell Host Microbe **6**:409–421.
27. **Lebkowski JS, Clancy S, Calos MP.** 1985. Simian virus 40 replication in adenovirus-transformed human cells antagonizes gene expression. Nature **317**:169–171.
28. **Kimpton J, Emerman M.** 1992. Detection of replication-competent and pseudotyped human immunodeficiency virus with a sensitive cell line on the basis of activation of an integrated beta-galactosidase gene. J. Virol. **66**:2232–2239.
29. **Nomaguchi M, Doi N, Fujiwara S, Fujita M, Adachi A.** 2010. Site-

directed mutagenesis of HIV-1 *vpu* gene demonstrates two clusters of replication-defective mutants with distinct ability to down-modulate cell surface CD4 and tetherin. Front. Microbiol. **1**:116. doi:10.3389/fmicb.2010.00116.
30. **McNatt MW, Zang T, Hatziioannou T, Bartlett M, Fofana IB, Johnson WE, Neil SJ, Bieniasz PD.** 2009. Species-specific activity of HIV-1 Vpu and positive selection of tetherin transmembrane domain variants. PLoS Pathog. **5**:e1000300. doi:10.1371/journal.ppat.1000300.
31. **Yoshida T, Kao S, Strebel K.** 2011. Identification of residues in the BST-2 TM domain important for antagonism by HIV-1 Vpu using a gain-of-function approach. Front. Microbiol. **2**:35. doi:10.3389/fmicb.2011.00035.
32. **Adachi A, Gendelman HE, Koenig S, Folks T, Willey R, Rabson A, Martin MA.** 1986. Production of acquired immunodeficiency syndrome-associated retrovirus in human and nonhuman cells transfected with an infectious molecular clone. J. Virol. **59**:284–291.
33. **Willey RL, Smith DH, Lasky LA, Theodore TS, Earl PL, Moss B, Capon DJ, Martin MA.** 1988. In vitro mutagenesis identifies a region within the envelope gene of the human immunodeficiency virus that is critical for infectivity. J. Virol. **62**:139–147.
34. **O'Doherty U, Swiggard WJ, Malim MH.** 2000. Human immunodeficiency virus type 1 spinoculation enhances infection through virus binding. J. Virol. **74**:10074–10080.
35. **Wilson SJ, Webb BL, Ylinen LM, Verschoor E, Heeney JL, Towers GJ.** 2008. Independent evolution of an antiviral TRIMCyp in rhesus macaques. Proc. Natl. Acad. Sci. U. S. A. **105**:3557–3562.
36. **Kono K, Song H, Yokoyama M, Sato H, Shioda T, Nakayama EE.** 2010. Multiple sites in the N-terminal half of simian immunodeficiency virus capsid protein contribute to evasion from rhesus monkey TRIM5α-mediated restriction. Retrovirology **7**:72. doi:10.1186/1742-4690-7-72.
37. **Howard BR, Vajdos FF, Li S, Sundquist WI, Hill CP.** 2003. Structural insights into the catalytic mechanism of cyclophilin A. Nat. Struct. Biol. **10**:475–481.
38. **Park SH, Mrse AA, Nevzorov AA, Mesleh MF, Oblatt-Montal M, Montal M, Opella SJ.** 2003. Three-dimensional structure of the channel-forming trans-membrane domain of virus protein "u" (Vpu) from HIV-1. J. Mol. Biol. **333**:409–424.
39. **Leaver-Fay A, Tyka M, Lewis SM, Lange OF, Thompson J, Jacak R, Kaufman K, Renfrew PD, Smith CA, Sheffler W, Davis IW, Cooper S, Treuille A, Mandell DJ, Richter F, Ban YE, Fleishman SJ, Corn JE, Kim DE, Lyskov S, Berrondo M, Mentzer S, Popović Z, Havranek JJ, Karanicolas J, Das R, Meiler J, Kortemme T, Gray JJ, Kuhlman B, Baker D, Bradley P.** 2011. ROSETTA3: an object-oriented software suite for the simulation and design of macromolecules. Methods Enzymol. **487**:545–574.
40. **Kirmaier A, Wu F, Newman RM, Hall LR, Morgan JS, O'Connor S, Marx PA, Meythaler M, Goldstein S, Buckler-White A, Kaur A, Hirsch VM, Johnson WE.** 2010. *TRIM5* suppresses cross-species transmission of a primate immunodeficiency virus and selects for emergence of resistant variants in the new species. PLoS Biol. **8**:e1000462. doi:10.1371/journal.pbio.1000462.
41. **Newman RM, Hall L, Connole M, Chen GL, Sato S, Yuste E, Diehl W, Hunter E, Kaur A, Miller GM, Johnson WE.** 2006. Balancing selection and the evolution of functional polymorphism in Old World monkey TRIM5alpha. Proc. Natl. Acad. Sci. U. S. A. **103**:19134–19139.
42. **Price AJ, Marzetta F, Lammers M, Ylinen LM, Schaller T, Wilson SJ, Towers GJ, James LC.** 2009. Active site remodeling switches HIV specificity of antiretroviral TRIMCyp. Nat. Struct. Mol. Biol. **16**:1036–1042.
43. **Ylinen LM, Price AJ, Rasaiyaah J, Hué S, Rose NJ, Marzetta F, James LC, Towers GJ.** 2010. Conformational adaptation of Asian macaque TRIMCyp directs lineage specific antiviral activity. PLoS Pathog. **6**:e1001062. doi:10.1371/journal.ppat.1001062.
44. **Fassati A.** 2012. Multiple roles of the capsid protein in the early steps of HIV-1 infection. Virus Res. **170**:15–24.
45. **Ganser-Pornillos BK, Yeager M, Sundquist WI.** 2008. The structural biology of HIV assembly. Curr. Opin. Struct. Biol. **18**:203–217.
46. **Miyamoto T, Yokoyama M, Kono K, Shioda T, Sato H, Nakayama EE.** 2011. A single amino acid of human immunodeficiency virus type 2 capsid protein affects conformation of two external loops and viral sensitivity to TRIM5α. PLoS One **6**:e22779. doi:10.1371/journal.pone.0022779.
47. **Nomaguchi M, Doi N, Fujiwara S, Saito A, Akari H, Nakayama EE, Shioda T, Yokoyama M, Sato H, Adachi A.** 2013. Systemic biological analysis of the mutations in two distinct HIV-1mt genomes occurred during replication in macaque cells. Microbes Infect. **15**:319–328.
48. **Hatziioannou T, Cowan S, Von Schwedler UK, Sundquist WI, Bieniasz PD.** 2004. Species-specific tropism determinants in the human immunodeficiency virus type 1 capsid. J. Virol. **78**:6005–6012.
49. **Owens CM, Song B, Perron MJ, Yang PC, Stremlau M, Sodroski J.** 2004. Binding and susceptibility to postentry restriction factors in monkey cells are specified by distinct regions of the human immunodeficiency virus type 1 capsid. J. Virol. **78**:5423–5437.
50. **von Schwedler UK, Stray KM, Garrus JE, Sundquist WI.** 2003. Functional surfaces of the human immunodeficiency virus type 1 capsid protein. J. Virol. **77**:5439–5450.
51. **Lim SY, Rogers T, Chan T, Whitney JB, Kim J, Sodroski J, Letvin NL.** 2010. TRIM5alpha modulates immunodeficiency virus control in rhesus monkeys. PLoS Pathog. **6**:e1000738. doi:10.1371/journal.ppat.1000738.
52. **Jia B, Serra-Moreno R, Neidermyer W, Rahmberg A, Mackey J, Fofana IB, Johnson WE, Westmoreland S, Evans DT.** 2009. Species-specific activity of SIV Nef and HIV-1 Vpu in overcoming restriction by tetherin/BST2. PLoS Pathog. **5**:e1000429. doi:10.1371/journal.ppat.1000429.
53. **Zhang F, Wilson SJ, Landford WC, Virgen B, Gregory D, Johnson MC, Munch J, Kirchhoff F, Bieniasz PD, Hatziioannou T.** 2009. Nef proteins from simian immunodeficiency viruses are tetherin antagonists. Cell Host Microbe **6**:54–67.
54. **Vigan R, Neil SJ.** 2010. Determinants of tetherin antagonism in the transmembrane domain of the human immunodeficiency virus type 1 Vpu protein. J. Virol. **84**:12958–12970.
55. **McCarthy KR, Schmidt AG, Kirmaier A, Wyand AL, Newman RM, Johnson WE.** 2013. Gain-of-sensitivity mutations in a Trim5-resistant primary isolate of pathogenic SIV identify two independent conserved determinants of Trim5α specificity. PLoS Pathog. **9**:e1003352. doi:10.1371/journal.ppat.1003352.
56. **Kuroishi A, Saito A, Shingai Y, Shioda T, Nomaguchi M, Adachi A, Akari H, Nakayama EE.** 2009. Modification of a loop sequence between alpha-helices 6 and 7 of virus capsid (CA) protein in a human immunodeficiency virus type 1 (HIV-1) derivative that has simian immunodeficiency virus (SIVmac239) vif and CA alpha-helices 4 and 5 loop improves replication in cynomolgus monkey cells. Retrovirology **6**:70. doi:10.1186/1742-4690-6-70.
57. **Ohkura S, Goldstone DC, Yap MW, Holden-Dye K, Taylor IA, Stoye JP.** 2011. Novel escape mutants suggest an extensive TRIM5α binding site spanning the entire outer surface of the murine leukemia virus capsid protein. PLoS Pathog. **7**:e1002011. doi:10.1371/journal.ppat.1002011.
58. **Homann S, Smith D, Little S, Richman D, Guatelli J.** 2011. Upregulation of BST-2/tetherin by HIV infection *in vivo*. J. Virol. **85**:10659–10668.
59. **Liberatore RA, Bieniasz PD.** 2011. Tetherin is a key effector of the antiretroviral activity of type I interferon in vitro and in vivo. Proc. Natl. Acad. Sci. U. S. A. **108**:18097–18101.
60. **Pillai SK, Abdel-Mohsen M, Guatelli J, Skasko M, Monto A, Fujimoto K, Yukl S, Greene WC, Kovari H, Rauch A, Fellay J, Battegay M, Hirschel B, Witteck A, Bernasconi E, Ledergerber B, Günthard HF, Wong JK,** Swiss HIV Cohort Study. 2012. Role of retroviral restriction factors in the interferon-α-mediated suppression of HIV-1 in vivo. Proc. Natl. Acad. Sci. U. S. A. **109**:3035–3040.
61. **Serra-Moreno R, Jia B, Breed M, Alvarez X, Evans DT.** 2011. Compensatory changes in the cytoplasmic tail of gp41 confer resistance to tetherin/BST-2 in a pathogenic nef-deleted SIV. Cell Host Microbe **9**:46–57.
62. **Goldstein S, Brown CR, Dehghani H, Lifson JD, Hirsch VM.** 2000. Intrinsic susceptibility of rhesus macaque peripheral CD4(+) T cells to simian immunodeficiency virus in vitro is predictive of in vivo viral replication. J. Virol. **74**:9388–9395.
63. **Lifson JD, Nowak MA, Goldstein S, Rossio JL, Kinter A, Vasquez G, Wiltrout TA, Brown C, Schneider D, Wahl L, Lloyd AL, Williams J, Elkins WR, Fauci AS, Hirsch VM.** 1997. The extent of early viral replication is a critical determinant of the natural history of simian immunodeficiency virus infection. J. Virol. **71**:9508–9514.
64. **Igarashi T, Iyengar R, Byrum RA, Buckler-White A, Dewar RL, Buckler CE, Lane HC, Kamada K, Adachi A, Martin MA.** 2007. Human immunodeficiency virus type 1 derivative with 7% simian immunodeficiency virus genetic content is able to establish infections in pig-tailed macaques. J. Virol. **81**:11549–11552.
65. **Lifson JD, Haigwood NL.** 2012. Lessons in nonhuman primate models for AIDS vaccine research: from minefields to milestones. Cold Spring Harb. Perspect. Med. **2**:a007310. doi:10.1101/cshperspect.a007310.
66. **Shaw GM, Hunter E.** 2012. HIV transmission. Cold Spring Harb. Perspect. Med. **2**:a006965. doi:10.1101/cshperspect.a006965.

67. **Swanstrom R, Coffin J.** 2012. HIV-1 pathogenesis: the virus. Cold Spring Harb. Perspect. Med. 2:a007443. doi:10.1101/cshperspect.a007443.
68. **Nishimura Y, Shingai M, Willey R, Sadjadpour R, Lee WR, Brown CR, Brenchley JM, Buckler-White A, Petros R, Eckhaus M, Hoffman V, Igarashi T, Martin MA.** 2010. Generation of the pathogenic R5-tropic simian/human immunodeficiency virus $SHIV_{AD8}$ by serial passaging in rhesus macaques. J. Virol. 84:4769–4781.
69. **Ren W, Mumbauer A, Gettie A, Seaman MS, Russell-Lodrigue K, Blanchard J, Westmoreland S, Cheng-Mayer C.** 2013. Generation of lineage-related, mucosally transmissible subtype C R5 simian-human immunodeficiency viruses capable of AIDS development, induction of neurological disease, and coreceptor switching in rhesus macaques. J. Virol. 87:6137–6149.
70. **Shingai M, Donau OK, Schmidt SD, Gautam R, Plishka RJ, Buckler-White A, Sadjadpour R, Lee WR, LaBranche CC, Montefiori DC, Mascola JR, Nishimura Y, Martin MA.** 2012. Most rhesus macaques infected with the CCR5-tropic $SHIV_{AD8}$ generate cross-reactive antibodies that neutralize multiple HIV-1 strains. Proc. Natl. Acad. Sci. U. S. A. 109:19769–19774.
71. **Shibata R, Kawamura M, Sakai H, Hayami M, Ishimoto A, Adachi A.** 1991. Generation of a chimeric human and simian immunodeficiency virus infectious to monkey peripheral blood mononuclear cells. J. Virol. 65:3514–3520.
72. **Kawamura M, Sakai H, Adachi A.** 1994. Human immunodeficiency virus Vpx is required for the early phase of replication in peripheral blood mononuclear cells. Microbiol. Immunol. 38:871–878.
73. **Gamble TR, Vajdos FF, Yoo S, Worthylake DK, Houseweart M, Sundquist WI, Hill CP.** 1996. Crystal structure of human cyclophilin A bound to the amino-terminal domain of HIV-1 capsid. Cell 87:1285–1294.

Journal of General Virology (2013), **94**, 2710–2716 DOI 10.1099/vir.0.055590-0

Short Communication

Generation of a replication-competent simian–human immunodeficiency virus, the neutralization sensitivity of which can be enhanced in the presence of a small-molecule CD4 mimic

Hiroyuki Otsuki,[1] Takayuki Hishiki,[1] Tomoyuki Miura,[1] Chie Hashimoto,[2] Tetsuo Narumi,[2] Hirokazu Tamamura,[2] Kazuhisa Yoshimura,[3] Shuzo Matsushita[4] and Tatsuhiko Igarashi[1]

Correspondence
Tatsuhiko Igarashi
tigarash@virus.kyoto-u.ac.jp

[1]Laboratory of Primate Model, Experimental Research Center for Infectious Diseases, Institute for Virus Research, Kyoto University, Kyoto 606-8507, Japan

[2]Department of Medicinal Chemistry, Institute of Biomaterials and Bioengineering, Tokyo Medical and Dental University, Tokyo 101-0062, Japan

[3]AIDS Research Center, National Institute of Infectious Diseases, Tokyo 162-8640, Japan

[4]Division of Clinical Retrovirology and Infectious Diseases, Center for AIDS Research, Kumamoto University, Kumamoto 860-0811, Japan

Simian–human immunodeficiency virus (SHIV) carrying the envelope from the clade B clinical human immunodeficiency virus type 1 (HIV-1) isolate MNA, designated SHIV MNA, was generated through intracellular homologous recombination. SHIV MNA inherited biological properties from the parental HIV-1, including CCR5 co-receptor preference, resistance to neutralization by the anti-V3 loop mAb KD-247 and loss of resistance in the presence of the CD4-mimic small-molecule YYA-021. SHIV MNA showed productive replication in rhesus macaque PBMCs. Experimental infection of a rhesus macaque with SHIV MNA caused a transient but high titre of plasma viral RNA and a moderate antibody response. Immunoglobulin in the plasma at 24 weeks post-infection was capable of neutralizing SHIV MNA in the presence but not in the absence of YYA-021. SHIV MNA could serve a model for development of novel therapeutic interventions based on CD4-mimic-mediated conversion of envelope protein susceptible to antibody neutralization.

Received 29 May 2013
Accepted 10 September 2013

Control of primate lentiviral infection by antibodies directed against viral envelope protein is theoretically feasible. This was confirmed by the successful protection of macaque monkeys from challenge inoculation with simian–human immunodeficiency virus (SHIV) carrying an envelope protein (Env). Env was derived from a laboratory strain of human immunodeficiency virus type 1 (HIV-1) through the passive immunization of neutralizing mAbs directed against HIV-1 (Mascola *et al.*, 2000; Nishimura *et al.*, 2003). This neutralization is consistent with the results normally seen in cell culture systems.

In contrast, clinical isolates of HIV-1 that have not been subjected to extensive passage in T-cell lines are generally resistant to antibody-mediated neutralization (Moore *et al.*, 1995). It has been shown that virus in infected individuals is under selective pressure to develop a variety of means to evade attack by neutralizing antibodies, including sequence variation, glycosylation, tertiary structural shielding formed by the Env trimer and the rapid kinetics of conformational changes of Env, which affect fusion between the viral envelope and the plasma membrane of target cells (Kong & Sattentau, 2012). Although four major neutralizing epitopes have been identified in HIV-1 Env (i.e. the V1/V2 loop, the glycan-V3 site and CD4-binding site of gp120, and the membrane-proximal external region of gp41), for reasons that are as yet unclear few reports of antibodies directed against these epitopes capable of neutralizing a broad range of isolates have been published (Kwong & Mascola, 2012). High titres of antibodies directed against the V3 loop are elicited in individuals during the early phase of HIV-1 infection, but these are incapable of neutralizing the virus because the epitope in functional Env trimer is probably shielded from the antibody (Davis *et al.*, 2009b). Therefore, it is necessary to develop a means of rendering these epitopes accessible to

One supplementary table and five supplementary figures are available with the online version of this paper.

the antibodies, to make antibody-mediated suppression of HIV-1 a valid therapeutic option.

It has been reported that neutralization mediated by antibodies directed against the V3 loop (Lusso *et al.*, 2005) or CD4-induced epitope (CD4i) (Thali *et al.*, 1993) can be enhanced in the presence of soluble CD4 (sCD4). It is known that the interaction of Env with sCD4 drives a conformational change of the viral protein and makes the cryptic/occult epitopes accessible to these antibodies (Wyatt *et al.*, 1998). Small molecules that emulate sCD4 for its interaction and subsequent induction of conformational change of Env may be employed to intensify antibody-mediated interventions against HIV-1 infection. Compounds with the above-mentioned properties (i.e. NBD-556 and NBD-557) have been reported previously (Zhao *et al.*, 2005). NBD-556 has been shown in cell culture to interact with the CD4-binding pocket to induce a conformational change in gp120 (Madani *et al.*, 2008) and enhance exposure of the Env of primary HIV-1 isolates to neutralizing epitopes (Yoshimura *et al.*, 2010).

The present study was performed to evaluate small-molecule CD4-mimic-based enhancement of antibody-mediated virus neutralization, in the context of virus infection *in vivo*. The SHIV/macaque monkey model of AIDS is particularly suitable for such studies, as SHIV carries the HIV-1 Env and the neutralization sensitivity of SHIV is comparable to that of the parental HIV-1 (Shibata & Adachi, 1992).

As NBD-556, unlike sCD4, inhibits infection with select HIV-1 isolates (Yoshimura *et al.*, 2010), we generated a new SHIV strain carrying Env, the sensitivity of which to antibody-mediated neutralization is enhanced in the presence of a CD4 mimic. An HIV-1 isolate (MNA), previously designated primary isolate HIV-1 Pt.3, was used as the source of Env, as the viral protein has been reported to interact with NBD-556 (Yoshimura *et al.*, 2010). While the virus belongs to a distinct subset of HIV-1 isolates, as mentioned above, it has also been reported to utilize the CCR5 molecule to gain entry into target cells, a property that is shared by the majority of HIV-1 strains (Yoshimura *et al.*, 2010). A mAb directed against the tip of the V3 loop (GPGR motif), KD-247 (Eda *et al.*, 2006), was employed to assess this concept, as HIV-1 MNA is resistant to KD-247-mediated neutralization, despite carrying the exact epitope sequence in the tip of the V3 loop, and is converted to being sensitive to the antibody by NBD-556 in a dose-dependent manner (Yoshimura *et al.*, 2010).

First, we reproduced the results of Yoshimura *et al.* (2010) using a neutralization assay employing TZM-bl cells (Platt *et al.*, 1998), obtained from the National Institutes of Health (NIH) AIDS Reagent Program (Fig. S1, available in JGV Online). The virus was resistant to KD-247, as described previously, and required almost 50 μg ml^{-1} of the antibody to achieve 50 % neutralization in our assay. However, the observed resistance was eliminated in the presence of 2 μM NBD-556; 50 % neutralization was achieved in the presence of ~0.1 μg KD-247 ml^{-1}, corresponding to 1/500 of the amount of the antibody to achieve the same degree of neutralization in the absence of the CD4 mimic.

With reproduction of the properties of HIV-1 MNA Env, we generated an SHIV strain carrying Env through intracellular homologous recombination, as described previously (Fujita *et al.*, 2013) with minor modifications (Fig. S2). DNA fragments representing the 5′ and 3′ ends of the SHIV genome (fragments I and II, respectively) were amplified by PCR from the proviral DNA plasmid SHIV KS661. A DNA fragment containing *env* (fragment III) was amplified from cDNA of the HIV-1 MNA genome, which was prepared from virus particles (virion-associated RNA) in the culture supernatant of PM1/CCR5 cells (Yusa *et al.*, 2005) infected with the virus. The PCR primers used are listed in Table S1. Using a FuGENE HD transfection reagent, lipofection was performed on the C8166-CCR5 cells (Shimizu *et al.*, 2006) to co-transfect them with 0.2 μg DNA. A cytopathic effect, presumably caused by the emerged recombinant virus, was observed on day 13 post-transfection. The emerged virus, designated SHIV MNA, carried the entire gp120 and three-quarters of gp41 from HIV-1 MNA Env (Fig. 1a). The rest of Env was from SHIV KS661, the Env of which was derived from HIV-1 89.6 (Shinohara *et al.*, 1999). The CD4 binding site, and the regions and elements that reportedly interact with NBD-556 (Madani *et al.*, 2008; Yoshimura *et al.*, 2010), are preserved in SHIV MNA Env (Fig. S3). The virus was replication competent in PM1/CCR5 cells (data not shown).

As HIV-1 MNA has been suggested to be a CCR5-utilizing virus, we were intrigued as to whether SHIV MNA inherited the trait from the parental virus. We subjected SHIV MNA and the parental HIV-1 MNA to a co-receptor usage assay as described previously (Nishimura *et al.*, 2010), with minor modifications (Fig. S4). As expected, SHIV MNA was shown to utilize CCR5 as an entry co-receptor.

We next assessed the neutralization profiles of SHIV MNA in comparison with the parental HIV-1 MNA, as described previously (Li *et al.*, 2005; Wei *et al.*, 2002). Both SHIV MNA and HIV-1 MNA showed essentially no neutralization by KD-247 up to 25 μg ml^{-1}, and 50 % neutralization was achieved at 50 μg ml^{-1} (Fig. 1b). As the CD4 mimic, we employed YYA-021, a compound generated and characterized through studies concerning the structure–activity relationships of small molecules (Narumi *et al.*, 2010, 2011, 2013; Yamada *et al.*, 2010). The compound was shown to be slightly less potent but to exhibit substantially lower toxicity than NBD-556, and was therefore a suitable choice for our purposes in future studies in animal models. SHIV MNA was resistant to neutralization by YYA-021 at all concentrations examined, except 25 and 50 μM, and showed a neutralization profile almost identical to that of HIV-1 MNA (Fig. 1c). To further characterize the

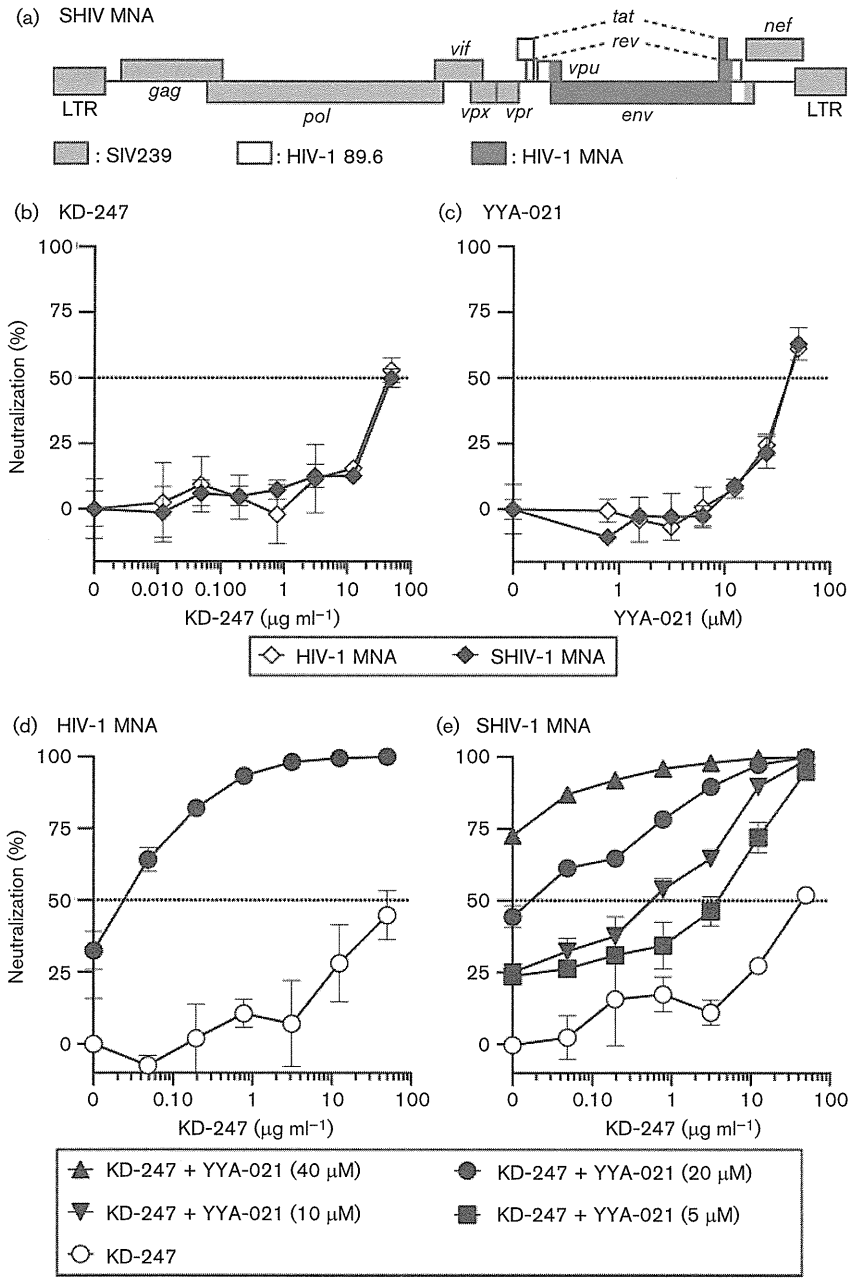

Fig. 1. Genomic organization (a) and neutralization sensitivity (b–e) of SHIV MNA. (a) Grey shaded boxes represent genes derived from SIV239, open boxes those from HIV-1 89.6 and dark grey shaded boxes those from HIV-1 MNA. LTR, long terminal repeat. (b–e) Percentage neutralization was calculated as 100×[1−(RLU.N−RLU.B)/(RLU.V−RLU.B)], where RLU is relative luciferase units; RLU.N is RLU in wells with cells, virus and KD-247 and/or YYA-021; RLU.V is RLU in wells with cells and virus; and RLU.B is RLU in wells with cells.

biological properties of SHIV MNA Env, a set of entry assays was conducted (Fig. S5). The *env* genes cloned from SHIV MNA and HIV-1 MNA were utilized to generate pseudotyped viruses. These pseudotypes were inoculated into TZM-bl cells in the presence of increasing amounts of NBD-556, YYA-021 or sCD4. A control group was derived from another virus preparation pseudotyped with amphotropic murine leukemia virus (A-MLV) Env (Landau *et al.*, 1991). When the efficiency of entry was defined by intracellular luciferase activities, virtually no difference was observed between Envs of SHIV MNA and the parental HIV-1. Thus, SHIV MNA Env replicated in

C8166-CCR5 cells retained sensitivity to small-molecule CD4 mimics and sCD4 comparable to that of HIV-1 MNA.

We then examined whether the synergistic neutralization of HIV-1 MNA by KD-247 antibody in the presence of NBD-556 (Yoshimura *et al.*, 2010) would be reproduced when CD4 mimic was substituted by YYA-021. The synergistic neutralization effect of KD-247 and YYA-021 was reproduced in our experiments (Fig. 1d). At 50 μg ml^{-1}, KD-247 barely achieved 50 % neutralization of HIV-1 MNA but resulted in 50 % neutralization at <0.05 μg ml^{-1} in the presence of 20 μM of YYA-021.

Finally, to examine whether these two agents neutralized SHIV MNA in the same manner as the parental HIV-1, we conducted a neutralization assay with KD-247 in the presence of increasing amounts of YYA-021 (0, 5, 10, 20 and 40 μM) (Fig. 1e). The neutralization curve of KD-247 against SHIV MNA showed an upward shift as the concentration of YYA-021 increased (Fig. 1e), similar to the observations with HIV-1 (Fig. 1d), indicating augmentation of neutralization, and complete neutralization of both viruses was achieved at 20 μM YYA-021 (Fig. 1d, e). Based on these results, we concluded that the neutralization profile of SHIV MNA was comparable to that of HIV-1 MNA.

Reproduction of the neutralization characteristics of HIV-1 MNA in the newly generated SHIV prompted us to assess the ability of SHIV MNA to replicate in monkey cells. SHIV MNA, along with SIV239 and SHIV KS661, were normalized with infectious titres and inoculated into rhesus macaque PBMC preparations from four animals,

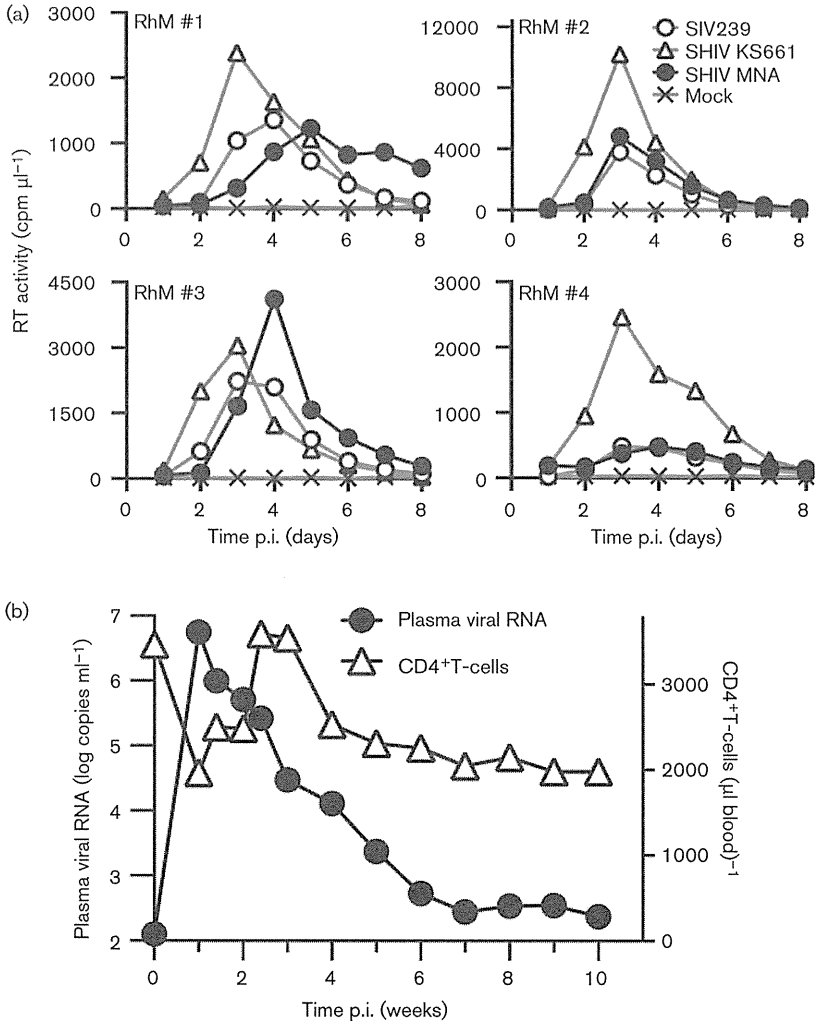

Fig. 2. Replication of SHIV MNA in rhesus macaque PBMCs (a) and *in vivo* (b). (a) M.o.i. was adjusted to 0.01 ($TCID_{50}$ per cell). (b) Experimental infection of a rhesus macaque with SHIV MNA. SHIV MNA (1.75×10^5 $TCID_{50}$) was intravenously inoculated into a rhesus macaque, and the plasma viral RNA burden and circulating $CD4^+$ T-lymphocytes were monitored.

as described previously (Fujita *et al.*, 2013) (Fig. 2a). SHIV KS661, a CXCR4-utilizing virus, replicated to the highest titres of all the viruses in all PBMC preparations. Compared with SHIV KS661, SIV239 replicated to lower titres. Under these experimental conditions, SHIV MNA showed productive replication in the cells with similar replication kinetics and peak titres to SIV239. Based on these results, we concluded that SHIV MNA was replication competent in primary monkey lymphocytes.

Productive replication of SHIV MNA in monkey PBMCs justified experimental infection of the virus *in vivo*. We inoculated 1.75×10^5 $TCID_{50}$ SHIV MNA intravenously into a rhesus macaque and monitored plasma viral RNA burden and circulating $CD4^+$ T-lymphocyte levels (Fig. 2b). Plasma viral RNA burden reached a peak of 5.6×10^6 copies ml^{-1} at 1 week post-infection (p.i.), and declined rapidly thereafter, reaching low levels of detection at 7 weeks p.i. (around 2.8×10^2 copies ml^{-1}). Circulating $CD4^+$ T-cell numbers showed a transient decrease around 1 week p.i., rebounded around 3 weeks p.i. and stabilized around 70 % of the pre-infection level from 4 weeks p.i. During the period of observation, the animal developed no obvious clinical manifestations related to lentivirus infection.

As SHIV MNA replicated *in vivo* without depleting helper T-cells, it was expected that the animal mounted an antiviral immune reaction. The production of antibody directed against Env was assessed by Western blotting, as described previously (Igarashi *et al.*, 1999). Purified Env protein (Advanced Biotechnologies) was used as the antigen (Fig. 3a). Anti-Env antibody was detected at 3 weeks p.i., and the level of antibody judged by the intensity of the band increased gradually with time.

We next examined whether the animal generated neutralizing antibodies against SHIV MNA. Because plasma samples from this specimen exhibited high background activity, IgG was purified from these samples collected on day 0 and in week 24 p.i. using protein G spin columns (GE Healthcare Japan). While the IgG from day 0 exhibited no neutralizing activity (Fig. 3b), as expected, the IgG collected at 24 weeks p.i. neutralized SHIV MNA, although a concentration >100 μg ml^{-1} was required to suppress replication of 100 $TCID_{50}$ of the input virus (Fig. 3c).

We examined whether the observed marginal neutralization by the antibody could be enhanced by the presence of YYA-021. Upon addition of YYA-021 in the assay system, SHIV MNA became sensitive to IgG obtained at 24 weeks p.i. (Fig. 3c), while no enhancement was identified from day 0 (Fig. 3b).

In this study, we generated a replication-competent SHIV MNA strain carrying an Env resistant to the neutralizing mAb KD-247 but conditionally sensitive in the presence of the CD4 mimic YYA-021. As the observed neutralization characteristics were identical to those of HIV-1 MNA, which contributed the majority of the Env sequence to the chimaera, the utility of the CD4 mimic as a means of enhancing antibody-mediated virus neutralization should be assessed in the context of infection *in vivo*. This concept could be tested during the acute phase of SHIV MNA infection, during which the virus undergoes substantial replication. To examine the feasibility of CD4-mimic-mediated enhancement of virus neutralization in the context of chronic infection, the conditions under which this type of intervention should be applied to HIV-1-infected patients in a clinical setting, the virus must be

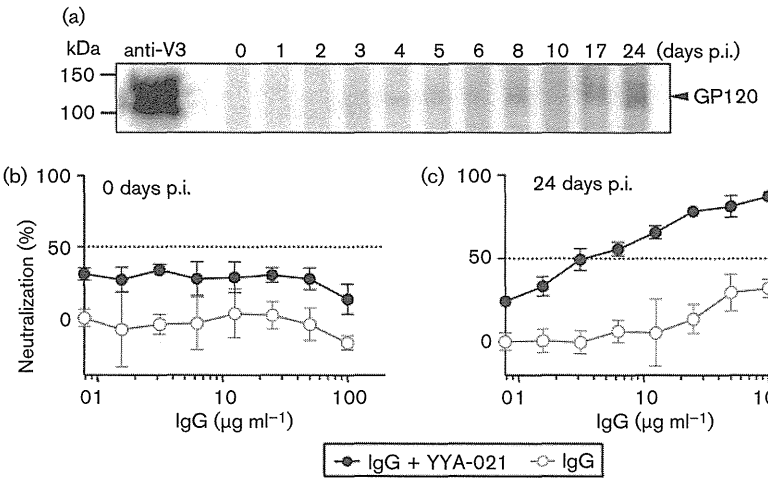

Fig. 3. Antibody induced against SHIV MNA. (a) The anti-HIV-1 gp120 antibody response was assessed by Western blotting with plasma samples collected at the indicated times. An anti-HIV-1 V3 mAb, 4G10 (ascites diluted 1 : 100) (von Brunn *et al.*, 1993), obtained from the NIH AIDS Reagent Program, was used as a positive control (lane anti-V3). (b, c) Neutralization of SHIV MNA with IgG purified from plasma of the infected rhesus macaque (day 0 and week 24 p.i.) with 20 μM YYA-021 or without YYA-021.

modified to sustain productive replication for a longer period. SHIV MNA in the present form does not fulfil this requirement. It is possible that animal-to-animal passage could increase the fitness of the virus in monkeys.

This study demonstrated that a CD4 mimic could modulate viral Env protein to be more susceptible to neutralization by less potent antibodies generated in the context of infection. During the early phase of infection, patients mount high titres of non-neutralizing antibodies directed against the V3 loop (Davis *et al.*, 2009a). Patients with HIV-1 clade C generate anti-Env antibodies, including anti-CD4i antibodies, with poor neutralizing activity against recent infection (Gray *et al.*, 2007). It is possible that the CD4 mimic YYA-021 causes a conformational change in SHIV MNA Env, which renders sequestered epitope(s) accessible to potentially neutralizing IgG, such as ones directed against the V3 loop and CD4i.

The current study extended the previous study by Yoshimura *et al.* (2010) and used HIV-1 MNA belonging to clade B to generate a new SHIV strain carrying Env. The neutralization sensitivity of this strain is characteristically augmented in the presence of a small-molecule CD4 mimic. Similar observations by Decker *et al.* (2005) showed that infections of a wide range of HIV-1 strains of multiple clades or circulating recombinant forms elicit high titres of anti-CD4i antibodies. These anti-CD4i antibodies neutralize viruses as divergent as HIV-2 in the presence of sCD4 (Decker *et al.*, 2005). Taking these observations into account, small-molecule CD4 mimics such as YYA-021 could potentially enhance the neutralization activity of the antibodies directed against autologous viruses belonging not only to clade B but also to multiple HIV-1 strains of various clades and possibly even HIV-2. Our results pave the way for a novel therapeutic intervention based on administration of CD4 mimics to patients with HIV to facilitate control of the virus by their own antibodies.

Acknowledgements

Thanks should be given to: Drs Julie Strizki and Paul Zavodny of the Schering-Plough Research Institute, Kenilworth, NJ, USA, for providing AD101; the NIH AIDS Research & Reference Reagent Program for providing TZM-bl cells, SV-A-MLV-env, 4G10 and soluble CD4; the Chemo-Sero-Therapeutic Research Institute, Kaketsuken, Japan, for providing mAb KD-247; former and current members of the Igarashi Laboratory for discussion and support. This work was supported by a Research on HIV/AIDS grant from the Ministry of Health, Labor and Welfare of Japan (H22-AIDS Research-007 and H24-AIDS Research-008) and by a Grant-in-Aid for Scientific Research (B) from the Japan Society for the Promotion of Science (23300156).

References

Davis, K. L., Bibollet-Ruche, F., Li, H., Decker, J. M., Kutsch, O., Morris, L., Salomon, A., Pinter, A., Hoxie, J. A. & other authors (2009a). Human immunodeficiency virus type 2 (HIV-2)/HIV-1 envelope chimeras detect high titers of broadly reactive HIV-1 V3-specific antibodies in human plasma. *J Virol* **83**, 1240–1259.

Davis, K. L., Gray, E. S., Moore, P. L., Decker, J. M., Salomon, A., Montefiori, D. C., Graham, B. S., Keefer, M. C., Pinter, A. & other authors (2009b). High titer HIV-1 V3-specific antibodies with broad reactivity but low neutralizing potency in acute infection and following vaccination. *Virology* **387**, 414–426.

Decker, J. M., Bibollet-Ruche, F., Wei, X., Wang, S., Levy, D. N., Wang, W., Delaporte, E., Peeters, M., Derdeyn, C. A. & other authors (2005). Antigenic conservation and immunogenicity of the HIV coreceptor binding site. *J Exp Med* **201**, 1407–1419.

Eda, Y., Takizawa, M., Murakami, T., Maeda, H., Kimachi, K., Yonemura, H., Koyanagi, S., Shiosaki, K., Higuchi, H. & other authors (2006). Sequential immunization with V3 peptides from primary human immunodeficiency virus type 1 produces cross-neutralizing antibodies against primary isolates with a matching narrow-neutralization sequence motif. *J Virol* **80**, 5552–5562.

Fujita, Y., Otsuki, H., Watanabe, Y., Yasui, M., Kobayashi, T., Miura, T. & Igarashi, T. (2013). Generation of a replication-competent chimeric simian-human immunodeficiency virus carrying env from subtype C clinical isolate through intracellular homologous recombination. *Virology* **436**, 100–111.

Gray, E. S., Moore, P. L., Choge, I. A., Decker, J. M., Bibollet-Ruche, F., Li, H., Leseka, N., Treurnicht, F., Mlisana, K. & other authors (2007). Neutralizing antibody responses in acute human immunodeficiency virus type 1 subtype C infection. *J Virol* **81**, 6187–6196.

Igarashi, T., Endo, Y., Englund, G., Sadjadpour, R., Matano, T., Buckler, C., Buckler-White, A., Plishka, R., Theodore, T. & other authors (1999). Emergence of a highly pathogenic simian/human immunodeficiency virus in a rhesus macaque treated with anti-CD8 mAb during a primary infection with a nonpathogenic virus. *Proc Natl Acad Sci U S A* **96**, 14049–14054.

Kong, L. & Sattentau, Q. J. (2012). Antigenicity and immunogenicity in HIV-1 antibody-based vaccine design. *J AIDS Clin Res* **S8**, 3.

Kwong, P. D. & Mascola, J. R. (2012). Human antibodies that neutralize HIV-1: identification, structures, and B cell ontogenies. *Immunity* **37**, 412–425.

Landau, N. R., Page, K. A. & Littman, D. R. (1991). Pseudotyping with human T-cell leukemia virus type I broadens the human immunodeficiency virus host range. *J Virol* **65**, 162–169.

Li, M., Gao, F., Mascola, J. R., Stamatatos, L., Polonis, V. R., Koutsoukos, M., Voss, G., Goepfert, P., Gilbert, P. & other authors (2005). Human immunodeficiency virus type 1 *env* clones from acute and early subtype B infections for standardized assessments of vaccine-elicited neutralizing antibodies. *J Virol* **79**, 10108–10125.

Lusso, P., Earl, P. L., Sironi, F., Santoro, F., Ripamonti, C., Scarlatti, G., Longhi, R., Berger, E. A. & Burastero, S. E. (2005). Cryptic nature of a conserved, CD4-inducible V3 loop neutralization epitope in the native envelope glycoprotein oligomer of CCR5-restricted, but not CXCR4-using, primary human immunodeficiency virus type 1 strains. *J Virol* **79**, 6957–6968.

Madani, N., Schön, A., Princiotto, A. M., Lalonde, J. M., Courter, J. R., Soeta, T., Ng, D., Wang, L., Brower, E. T. & other authors (2008). Small-molecule CD4 mimics interact with a highly conserved pocket on HIV-1 gp120. *Structure* **16**, 1689–1701.

Mascola, J. R., Stiegler, G., VanCott, T. C., Katinger, H., Carpenter, C. B., Hanson, C. E., Beary, H., Hayes, D., Frankel, S. S. & other authors (2000). Protection of macaques against vaginal transmission of a pathogenic HIV-1/SIV chimeric virus by passive infusion of neutralizing antibodies. *Nat Med* **6**, 207–210.

Moore, J. P., Cao, Y., Qing, L., Sattentau, Q. J., Pyati, J., Koduri, R., Robinson, J., Barbas, C. F., III, Burton, D. R. & Ho, D. D. (1995).

Primary isolates of human immunodeficiency virus type 1 are relatively resistant to neutralization by monoclonal antibodies to gp120, and their neutralization is not predicted by studies with monomeric gp120. *J Virol* **69**, 101–109.

Narumi, T., Ochiai, C., Yoshimura, K., Harada, S., Tanaka, T., Nomura, W., Arai, H., Ozaki, T., Ohashi, N. & other authors (2010). CD4 mimics targeting the HIV entry mechanism and their hybrid molecules with a CXCR4 antagonist. *Bioorg Med Chem Lett* **20**, 5853–5858.

Narumi, T., Arai, H., Yoshimura, K., Harada, S., Nomura, W., Matsushita, S. & Tamamura, H. (2011). Small molecular CD4 mimics as HIV entry inhibitors. *Bioorg Med Chem* **19**, 6735–6742.

Narumi, T., Arai, H., Yoshimura, K., Harada, S., Hirota, Y., Ohashi, N., Hashimoto, C., Nomura, W., Matsushita, S. & Tamamura, H. (2013). CD4 mimics as HIV entry inhibitors: lead optimization studies of the aromatic substituents. *Bioorg Med Chem* **21**, 2518–2526.

Nishimura, Y., Igarashi, T., Haigwood, N. L., Sadjadpour, R., Donau, O. K., Buckler, C., Plishka, R. J., Buckler-White, A. & Martin, M. A. (2003). Transfer of neutralizing IgG to macaques 6 h but not 24 h after SHIV infection confers sterilizing protection: implications for HIV-1 vaccine development. *Proc Natl Acad Sci U S A* **100**, 15131–15136.

Nishimura, Y., Shingai, M., Willey, R., Sadjadpour, R., Lee, W. R., Brown, C. R., Brenchley, J. M., Buckler-White, A., Petros, R. & other authors (2010). Generation of the pathogenic R5-tropic simian/human immunodeficiency virus SHIVAD8 by serial passaging in rhesus macaques. *J Virol* **84**, 4769–4781.

Platt, E. J., Wehrly, K., Kuhmann, S. E., Chesebro, B. & Kabat, D. (1998). Effects of CCR5 and CD4 cell surface concentrations on infections by macrophagetropic isolates of human immunodeficiency virus type 1. *J Virol* **72**, 2855–2864.

Shibata, R. & Adachi, A. (1992). SIV/HIV recombinants and their use in studying biological properties. *AIDS Res Hum Retroviruses* **8**, 403–409.

Shimizu, Y., Okoba, M., Yamazaki, N., Goto, Y., Miura, T., Hayami, M., Hoshino, H. & Haga, T. (2006). Construction and in vitro characterization of a chimeric simian and human immunodeficiency virus with the RANTES gene. *Microbes Infect* **8**, 105–113.

Shinohara, K., Sakai, K., Ando, S., Ami, Y., Yoshino, N., Takahashi, E., Someya, K., Suzaki, Y., Nakasone, T. & other authors (1999). A highly pathogenic simian/human immunodeficiency virus with genetic changes in cynomolgus monkey. *J Gen Virol* **80**, 1231–1240.

Thali, M., Moore, J. P., Furman, C., Charles, M., Ho, D. D., Robinson, J. & Sodroski, J. (1993). Characterization of conserved human immunodeficiency virus type 1 gp120 neutralization epitopes exposed upon gp120-CD4 binding. *J Virol* **67**, 3978–3988.

von Brunn, A., Brand, M., Reichhuber, C., Morys-Wortmann, C., Deinhardt, F. & Schödel, F. (1993). Principal neutralizing domain of HIV-1 is highly immunogenic when expressed on the surface of hepatitis B core particles. *Vaccine* **11**, 817–824.

Wei, X., Decker, J. M., Liu, H., Zhang, Z., Arani, R. B., Kilby, J. M., Saag, M. S., Wu, X., Shaw, G. M. & Kappes, J. C. (2002). Emergence of resistant human immunodeficiency virus type 1 in patients receiving fusion inhibitor (T-20) monotherapy. *Antimicrob Agents Chemother* **46**, 1896–1905.

Wyatt, R., Kwong, P. D., Desjardins, E., Sweet, R. W., Robinson, J., Hendrickson, W. A. & Sodroski, J. G. (1998). The antigenic structure of the HIV gp120 envelope glycoprotein. *Nature* **393**, 705–711.

Yamada, Y., Ochiai, C., Yoshimura, K., Tanaka, T., Ohashi, N., Narumi, T., Nomura, W., Harada, S., Matsushita, S. & Tamamura, H. (2010). CD4 mimics targeting the mechanism of HIV entry. *Bioorg Med Chem Lett* **20**, 354–358.

Yoshimura, K., Harada, S., Shibata, J., Hatada, M., Yamada, Y., Ochiai, C., Tamamura, H. & Matsushita, S. (2010). Enhanced exposure of human immunodeficiency virus type 1 primary isolate neutralization epitopes through binding of CD4 mimetic compounds. *J Virol* **84**, 7558–7568.

Yusa, K., Maeda, Y., Fujioka, A., Monde, K. & Harada, S. (2005). Isolation of TAK-779-resistant HIV-1 from an R5 HIV-1 GP120 V3 loop library. *J Biol Chem* **280**, 30083–30090.

Zhao, Q., Ma, L., Jiang, S., Lu, H., Liu, S., He, Y., Strick, N., Neamati, N. & Debnath, A. K. (2005). Identification of *N*-phenyl-*N'*-(2,2,6,6-tetramethyl-piperidin-4-yl)-oxalamides as a new class of HIV-1 entry inhibitors that prevent gp120 binding to CD4. *Virology* **339**, 213–225.

Bioorganic & Medicinal Chemistry 21 (2013) 7884–7889

Contents lists available at ScienceDirect

Bioorganic & Medicinal Chemistry

journal homepage: www.elsevier.com/locate/bmc

A CD4 mimic as an HIV entry inhibitor: Pharmacokinetics

Chie Hashimoto [a], Tetsuo Narumi [a], Hiroyuki Otsuki [b], Yuki Hirota [a], Hiroshi Arai [a], Kazuhisa Yoshimura [c,d], Shigeyoshi Harada [c,d], Nami Ohashi [a], Wataru Nomura [a], Tomoyuki Miura [b], Tatsuhiko Igarashi [b], Shuzo Matsushita [d], Hirokazu Tamamura [a,*]

[a] Institute of Biomaterials and Bioengineering, Tokyo Medical and Dental University, Chiyoda-ku, Tokyo 101-0062, Japan
[b] Institute for Virus Research, Kyoto University, Kyoto 606-8507, Japan
[c] AIDS Research Center, National Institute of Infectious Diseases, Shinjuku-ku, Tokyo 162-8640, Japan
[d] Center for AIDS Research, Kumamoto University, Kumamoto 860-0811, Japan

ARTICLE INFO

Article history:
Received 17 September 2013
Revised 5 October 2013
Accepted 5 October 2013
Available online 17 October 2013

Keywords:
CD4 mimic
HIV entry inhibitor
Intravenous administration
Pharmacokinetics

ABSTRACT

To date, several small molecules of CD4 mimics, which can suppress competitively the interaction between an HIV-1 envelope glycoprotein gp120 and a cellular surface protein CD4, have been reported as viral entry inhibitors. A lead compound **2** (YYA-021) with relatively high potency and low cytotoxicity has been identified previously by SAR studies. In the present study, the pharmacokinetics of the intravenous administration of compound **2** in rats and rhesus macaques is reported. The half-lives of compound **2** in blood in rats and rhesus macaques suggest that compound **2** shows wide tissue distribution and relatively high distribution volumes. A few hours after the injection, both plasma concentrations of compound **2** maintained micromolar levels, indicating it might have promise for intravenous administration when used combinatorially with anti-gp120 monoclonal antibodies.

1. Introduction

Several anti-HIV-1 drugs, including protease inhibitors and integrase inhibitors have been developed and have contributed to the highly active anti-retroviral therapy (HAART) used to treat AIDS.[1] Prevention of the HIV-1 infection of its target cells[1,2] is however a legitimate goal and the viral attachment process is an important target for the development of the drugs which could forestall such infection. The dynamic and supramolecular entry of human immunodeficiency virus type 1 (HIV-1) into target cells is initiated by the interaction of a viral envelope glycoprotein gp120 with the cell surface protein CD4.[3] Sequential binding of CD4 and a co-receptor (CCR5 or CXCR4) to gp120 can trigger a series of conformational rearrangements of gp41, a viral transmembrane glycoprotein mediating fusion between the viral and cellular membranes.[3–6] Control, especially of dynamic conformational changes of the envelope glycoproteins is a very attractive option.[7] To date, several small molecules that mimic CD4 have been developed as HIV-1 entry inhibitors, which competitively block the binding of gp120 to CD4[8] and the potential of these CD4 mimics has been explored (Fig. 1).[9–11] Furthermore, the interaction of CD4 mimics with a highly conserved pocket on gp120, designated as the 'Phe43 cavity', induces conformational changes in gp120,[12] a process which occurs with unfavorable binding entropy, and leads to a favorable enthalpy change similar to that caused by binding of the soluble CD4 binding to gp120. Thus, these unique properties render CD4 mimics valuable not only as entry inhibitors but also as 'envelope protein openers' and putatively, stimulants when combined with neutralizing antibodies.[13]

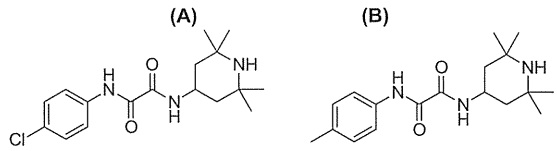

NBD-556 (**1**) YYA-021 (**2**)

Figure 1. Structures of NBD-556 (**1**) and YYA-021 (**2**).

Through our SAR studies a lead compound YYA-021 (**2**) with relatively high potency and low cytotoxicity has been found,[11] although the original compound NBD-556 (**1**) had relatively high cytotoxicity. Pharmacokinetic (PK) studies were performed to assess the potential of compound **2** for clinical application and in addition, the possibility and the effectiveness of its use in combination with neutralization antibodies are discussed.

* Corresponding author. Tel.: +81 3 5280 8036; fax: +81 3 5280 8039.
E-mail address: tamamura.mr@tmd.ac.jp (H. Tamamura).

0968-0896/$ - see front matter © 2013 Elsevier Ltd. All rights reserved.
http://dx.doi.org/10.1016/j.bmc.2013.10.005

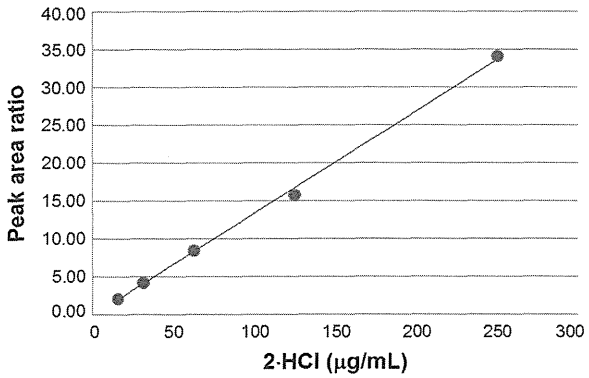

Figure 2. A calibration curve of compound **2·HCl** for calculating PK in rats.

2. Results and discussion

2.1. Calibration curve

Compound **2** was converted to its hydrochloride salt **2·HCl**, by treatment with 4 M HCl in dioxane. Standard solutions in saline of this HCl salt at concentrations over a range of 0–250 μg/mL were prepared and a calibration curve was constructed using the ratio of observed HPLC peak areas and concentrations of **2·HCl** to demonstrate the linearity shown in Figure 2.[14] The corresponding linear regression equation is $Y = 0.1345X$ ($R^2 = 0.9981$). Plasma concentrations of **2·HCl** were measured using this equation. The calibration curve shown in SD Figure S5C for the concentrations of compound **2** in plasma of a rhesus macaque was constructed using standard solutions of **2·HCl** in saline at concentrations over a range of 0–312.5 μg/mL. The linear regression equation in this case is $Y = 0.034X$ ($R^2 = 0.9927$). For adsorption of compound **2** by blood cells of a rhesus macaque, a calibration curve was constructed using standard solutions of **2·HCl** in saline at concentrations over a range of 0–950 μg/mL. The linear regression equation is $Y = 0.0553X$ ($R^2 = 0.9263$) and the curve is shown in SD Figure S7C.

2.2. Pharmacokinetics in rats

The primary stock solution of **2·HCl** was prepared in saline (2.5 mg/mL). Initially, the acute toxicity of compound **2** in rats was investigated to determine its maximum tolerated dose. The HCl salt, compound **2·HCl**, (0, 0.5, 1.0, 2.5 and 5.0 mg) was administered by tail vein injection into Jcl:SD rats (3 or 4 rats for each dose). Rats with the 5.0 mg administration showed a relatively low increase in the body weight although the intake amount of bait and water increased remarkably two weeks after administration, compared to the other rats (Supplementary data, SD Figs. S1 and S2). This observation suggested abnormalities such as renal and hepatic dysfunction and as a result, the maximum dose in rats of **2·HCl** was determined to be 2.5 mg.

Compound **2·HCl** (2.5 mg) in saline (1 mL) was administered at a level of 14 mg/kg by tail vein injection into Jcl:SD rats. Blood was collected from the tail vein into centrifugal blood collection tubes 15, 30, 45, 60, 120 and 240 min after administration of **2·HCl**. Plasma (50 μL) obtained from the blood sample was mixed with phenol in saline (final volume 60 μL) and centrifuged at 2000*g* for 3 min to remove any protein. The resultant supernatant was used in the analysis. A 50 μL aliquot of each filtrate was injected into HPLC by an autosampler. Compound **2** was detected in the HPLC analysis and was characterized by ESI-TOF-MS. The HPLC chart of the filtrate collected 30 min after administration of compound **2** is shown in Figure 3. Concentrations in blood of compound **2** after administration (15, 30, 45, 60, 120 and 240 min) were calculated using the calibration curve (SD Fig. S4) and plotted as shown in Figure 4.[15]

Using the data measured at 15, 30, 45, 60, 120 and 240 min, the half-life was calculated as 8.4 min by curve fitting with a one-compartment model based on GraphPad Prism Version 5.04 (GraphPad Software, CA, U.S.A). The initial concentration was calculated as 17.3 μg/mL. Compound **2** has a low molecular weight (317.4) and some level of hydrophobicity based on its structure, suggesting that the renal excretion is unlikely. At a dose of 2500 (μg)/initial concentration 17.3 (μg/mL), the volume of distribution was calculated as 145 mL, suggesting widespread tissue distribution of **2** as a result of its hydrophobicity.

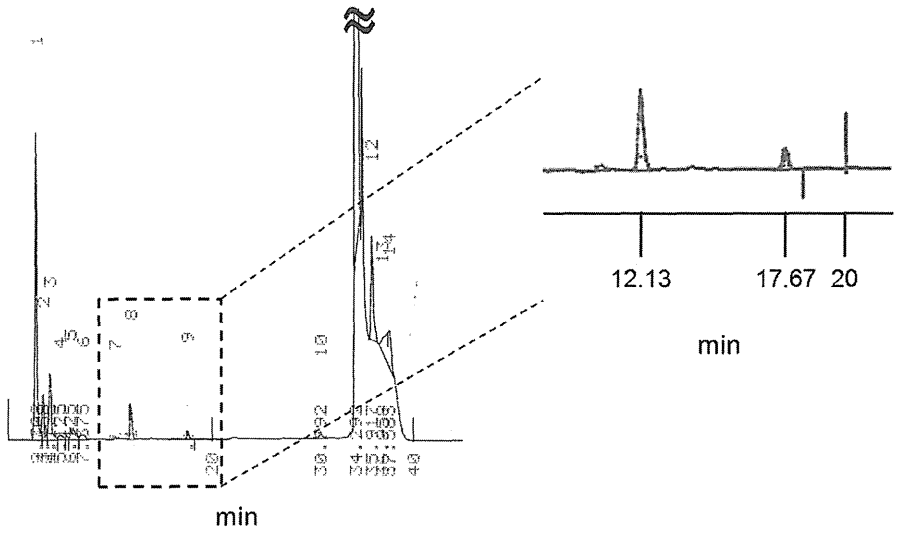

Figure 3. HPLC chart of rat plasma 30 min after intravenous administration of compound **2**. The plasma sample was eluted with a linear gradient of 20–35% CH_3CN (0.1% TFA, in 30 min). Peak 8 (retention time: 12.13 min) corresponds to the internal standard (phenol) and peak 9 (retention time: 17.67 min) corresponds to compound **2**.

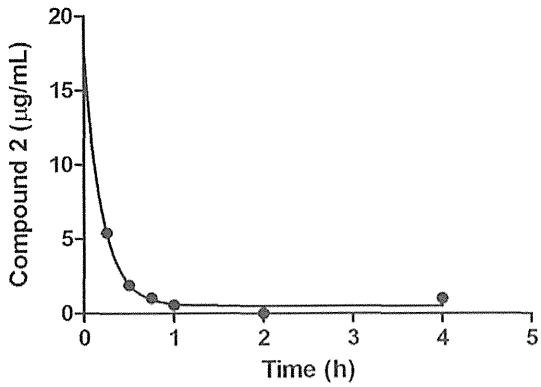

Figure 4. Plots of concentrations in rat blood of compound **2** after administration (15, 30, 45, 60, 120 and 240 min). Half-life is calculated as 0.141 h (8.4 min). The plasma of a representative rat was used for the analyses.

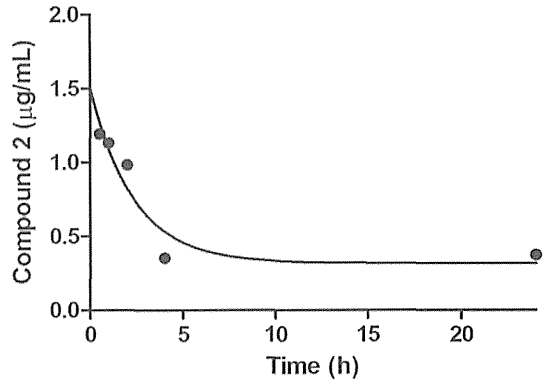

Figure 6. Plots of macaque blood concentrations of compound **2** after administration of **2·HCl** (0.5, 1, 2, 4 and 24 h). Half-life is calculated as 1.64 h (98.4 min). The plasma of a rhesus macaque was used for the analyses.

2.3. Pharmacokinetics in a rhesus macaque

The primary stock solution of the **2·HCl** was prepared in potassium-free phosphate-buffered saline (Na_2HPO_4 + NaH_2PO_4 + NaCl, pH 7.4) (2.4 mg/mL) to avoid hyperpotassemia and acidosis. Initially, the acute toxicity observed by treatment with **2·HCl** in a rhesus macaque was investigated to determine the maximum tolerated dose. **2·HCl** (14.1, 35.3 and 70.6 mg) was administered by cephalic vein injection into a rhesus macaque (one macaque for each dose). A macaque administered 70.6 mg, showed abnormalities such as mydriasis, prolonged PR interval in the electrocardiogram and bradycardia, while acute toxicity was not observed following the administration of **2·HCl** at levels up to 35.3 mg[16] and the maximum tolerated dose in a rhesus macaque was determined to be 35.3 mg (6.7 mg/kg). The macaque which had been administered 70.6 mg of **2·HCl** was treated by an emergency intervention with dobutamine (iv).

Compound **2·HCl** (70.6 mg) was intravenously administered at 13.4 mg/kg into a rhesus macaque. Blood (3.0 mL) was collected from cephalic vein 0, 0.5, 1, 2, 4 and 24 h after administration of the hydrochloride using winged needles. Plasma (60 μL) obtained from the blood sample was mixed with MeOH (200 μL) to remove plasma proteins and then centrifuged at 2000*g* for 3 min at room temperature in a microcentrifuge (MCF-2360, LMS Co., Ltd., Tokyo, Japan). A 228 μL aliquot of each supernatant was mixed with 12 μL of phenol in saline (stock solution: 0.3 mg/mL) to give a final concentration of phenol of 150 μg/mL, then filtered. A 200 μL aliquot of each filtrate was analyzed by HPLC using phenol as an internal standard. Compound **2** was detected in the HPLC analysis of each filtrate and its peak was characterized by ESI-TOF-MS. The HPLC of the filtrate prepared 30 min after administration of **2·HCl** is shown in Figure 5. Blood concentrations of compound **2** after 0.5, 1, 2, 4 or 24 h administration were calculated using the calibration curve (SD Fig. S6) and plotted as shown in Figure 6.

Using the time-course data, the half-life was calculated as 98.4 min by curve fitting based on GraphPad Prism Version 5.04 (GraphPad Software, CA, U.S.A.). The initial concentration in blood was also calculated as 1.50 μg/mL. In a macaque, this suggests that the renal excretion is not possible and this was by the absence of compound **2** in the HPLC analysis of the urine (SD). The distribution volume was calculated as 47.1 L; the dose 70.6 (mg)/initial concentration 1.50 (μg/mL) ratio suggests tissue distribution.

2.4. Adsorption of compound 2 to blood cells of a rhesus macaque

The question of whether compound **2** can be attached to and adsorbed into blood cells was investigated. Initially, **2·HCl** was added to blood (1 mL) of a rhesus macaque reaching a final concentration of 1 mg/mL. This mixture was incubated at 37 °C for 0, 1 and 2 h, and then centrifuged at 3600 rpm for 5 min at room temperature in a microcentrifuge to separate plasma (730 μL) from

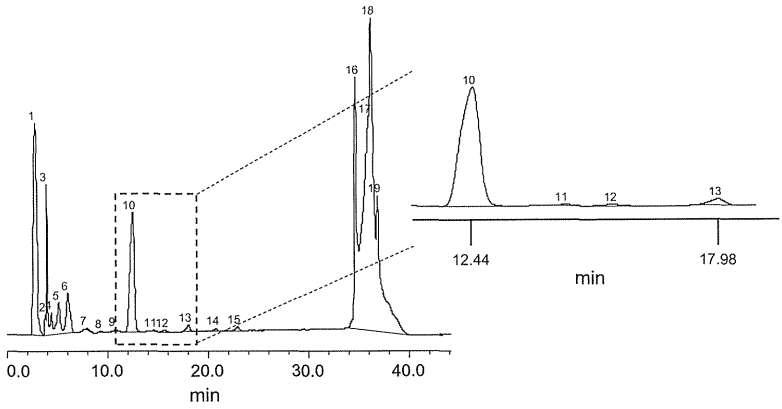

Figure 5. HPLC chart of macaque plasma 30 min after intravenous administration of **2·HCl**. The plasma sample was eluted with a linear gradient of 20–35% CH_3CN (0.1% TFA, in 30 min). Peak 10 (retention time: 12.44 min) corresponds to the internal standard (phenol) and peak 13 (retention time: 17.98 min) corresponds to compound **2**.

blood cells. In addition, plasma (0.5 mL) was added to the blood cells incubated for 1 h, then the mixture was incubated again for 1 h to separate plasma (730 μL) from the blood cells. Blood cell samples were prepared by mixing the blood cells with 480 μL of PBS and diluting the mixture to 1 mL with PBS. Blood cell samples were sonicated to disrupt cell membranes then both plasma and blood cell samples (60 μL each) were vortex-mixed with 200 μL of MeOH, then centrifuged at 2000*g* for 3 min at room temperature. A 228 μL aliquot of each supernatant was mixed with 12 μL of phenol in saline (final concentration: 600 μg/mL) and filtered. A 200 μL aliquot of each filtrate was injected to HPLC by an autosampler (SD Fig. S8).

The fractions of plasma and blood cells were analyzed by HPLC to quantify compound **2** (Fig. 7). The results showed that incubation enhanced the attachment or adsorption of compound **2** to blood cells; incubation for 1 or 2 h led to percentages of 39.7% and 39.3%, respectively, in distribution in cells, prior to incubation there was a distribution percentage of 34.8% in cells. Furthermore, compound **2**, which was adsorbed into blood cells, was significantly redistributed in plasma when fresh plasma was added; the addition of plasma to blood cells incubated for 1 h and a further incubation for 1 h caused redistribution of compound **2** to plasma and a reduction of distribution percentages to cells from 39.7% to 11.5%. This suggests that compound **2**, which was attached to blood cells, might be transferred from the cells to plasma and subsequently distributed to tissues.

These results indicate that the concentration in blood of compound **2** might be reduced, ultimately to ~1 mg/mL (3 μM) with 2–4 h treatments in rats (14 mg/kg) and rhesus macaques (13.4 mg/kg). The EC_{50} value of compound **2** has been determined as 10–50 μM in laboratory and primary HIV-1 strains.[11] Thus, in several hours after intravenous administration of compound **2** the efficacy might be diminished because the concentration in blood of compound **2** is being maintained below EC_{50} levels. However, the amount administered cannot be increased because of the acute toxicity which is described in the previous section, although the concentration in blood of compound **2** does not reach its CC_{50} level of 210 μM.[11] Recently, we reported that CD4 mimics such as compound **1** enhance the binding potency of anti-gp120 monoclonal antibodies such as KD-247[16] toward an envelope protein gp120, showing synergistic neutralization.[13] Compound **2** also enhances the neutralizing activity of KD-247 against simian–human immunodeficiency virus (SHIV)-KS661 strain via highly synergistic interactions. When compound **2** is used in combination with anti-gp120 monoclonal antibodies such as KD-247, the level of compound **2** of 3 μM might be sufficient for neutralization in vivo and thus it might be possible to reduce the dose of compound **2**. In addition, we also found that compound **1** and CXCR4 antagonists such as T140[2] showed synergistic anti-HIV-1 activity,[11] Thus, a combinatorial use with co-receptor antagonists would be also effective for reduction of the dose of compound **2**.

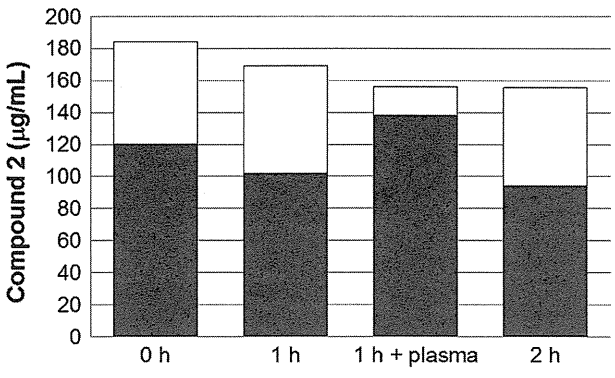

Figure 7. Quantitative analysis of compound **2** contained in macaque blood cells and plasma after incubation for 0, 1, or 2 h. 1 h + plasma means the addition of plasma (0.5 mL) to 1 h incubated blood cells followed by further incubation for 1 h. Concentrations of compound **2** in plasma are shown in black bars, and those in blood cells are shown in white bars.

3. Conclusion

CD4 mimics are attractive not only as HIV entry inhibitors but also possibly as cooperating agents for neutralizing antibodies. Binding of CD4 mimicking compounds to gp120 causes a conformational change in gp120. In this way, CD4 mimics function as 'envelope openers' and enhance the binding ability of anti-gp120 neutralizing antibodies. We discovered lead compound **2** with relatively high potency and low cytotoxicity in our previous study. In the current study, the pharmacokinetics of compound **2** in rats and rhesus macaques in the intravenous administration were investigated. Plots of plasma concentrations of compound **2** fitted with a one-compartment model provided calculation of half-lives of compound **2** in blood in rats and rhesus macaques: 8.4 and 98.4 min, respectively, suggesting that compound **2** is broadly distributed in tissues. A few hours post-injection, plasma concentrations of compound **2** in both species stabilized at micromolar levels. Consequently, compound **2** might have promise as a lead compound for the intravenous administration in a cocktail therapy with anti-gp120 monoclonal antibodies such as KD-247 and with co-receptor antagonists such as T140.[2]

4. Experimental

4.1. General information

A Cosmosil 5C18-ARII column (4.6 × 250 mm, Nacalai Tesque, Inc., Kyoto, Japan) was used for analytical HPLC, with a linear gradient of CH_3CN containing 0.1% (v/v) TFA at a flow rate of 1 cm^3 min^{-1} on a JASCO PU-2089 plus (JASCO Corporation, Ltd., Tokyo, Japan), and eluents were detected by UV at 220 nm on a JASCO UV-2075 plus (JASCO Corporation, Ltd, Tokyo, Japan). Samples were injected by an autosampler on a JASCO AS-2075 plus (JASCO Corporation, Ltd, Tokyo, Japan). ESI-TOF-MS were recorded on a micrOTOF-2focus (Bruker Daltonics) mass spectrometer.

4.2. Calibration curve

To compound **2** (1.0 g) in MeOH (5 mL) was added 4 M HCl/dioxane (10 mL) and the mixture was stirred for 30 min at room temperature. The mixture was concentrated under reduced pressure and the **2**·**HCl** was precipitated in cooled Et_2O (yield: 1.2 g, quantitative).

To construct a pharmacokinetics calibration curve in a rat, standard stock solutions in saline of **2**·**HCl**; 263, 131.5, 65.8, 32.9 and 16.4 μg/mL and an internal standard stock solution; 1.25 mg/mL phenol in saline were prepared. Each standard stock solution (22.8 μL) was mixed with 1.2 μL of the internal stock solution to give a total volume of 24 μL, then filtered. A 20 μL aliquot of each filtrate was injected to HPLC. The final concentration of **2**·**HCl** was 250, 125, 62.5, 31.3 or 15.6 μg/mL and each sample contains 62.5 μg/mL phenol. Elution was carried out with a linear gradient of 20–35% CH_3CN (0.1% TFA) over 30 min (SD Fig. S3). A calibration curve was constructed using the ratio of HPLC peak areas and concentrations of **2**·**HCl** to demonstrate the linearity as shown in Figure 2. The linear regression equation is $Y = 0.1345X$ ($R^2 = 0.9981$).

To construct a pharmacokinetics calibration curve in a rhesus macaque, standard stock solutions in saline of **2**·**HCl** (329, 164.5,